Electroweak Quantum Chemistry for Possible Precursor Molecules in the Evolution of Biomolecular Homochirality

by **Robert Berger**, **Martin Quack***, and **Gregory S. Tschumper**

Laboratorium für Physikalische Chemie, ETH-Zürich, ETH-Zentrum, CH-8092 Zürich

Dedicated to *Albert Eschenmoser* on the occasion of his 75th birthday

The unified 'electroweak' theory of the electromagnetic and weak nuclear interactions in physics predicts a small energy difference (ΔE_{pv}) between the left- and right-handed enantiomers of chiral molecules. Thus, electroweak theory provides one of several possible explanations for the origin of biomolecular homochirality (nature's preference for L-amino acids and D-monosaccharides). Recent systematic electroweak quantum-chemical studies find ΔE_{pv} to be an order of magnitude larger than previously anticipated, which has sparked renewed interest in the subject. The present paper addresses, for the first time, the question of the relative stability of certain possible prebiotic precursor molecules suggested in the work of *A. Eschenmoser* and co-workers: aziridine-2-carbonitrile ($CH_2NHCHCN$) and oxiranecarbonitrile (CH_2OCHCN), also commonly referred to as 2-cyanoaziridine and cyanooxirane, respectively. The *cis*/*trans*-isomerization pathway of aziridine-2-carbonitrile is initially characterized by standard quantum-chemical techniques. At the highest level of theory employed, the *trans*-isomer is found to lie by 4.0 kJ mol^{-1} above its *cis*-counterpart. The transition state connecting the two is another 74 kJ mol^{-1} higher in energy. After including unscaled, harmonic zero-point energy corrections, these values change to 3.7 and 69 kJ mol^{-1}, respectively. Using the multi-configuration linear response (MCLR) approach to electroweak quantum chemistry (R. Berger, M. Quack, *J. Chem. Phys.* **2000**, *112*, 3148), the energy difference between the enantiomers of the various compounds and transition structures has been computed within the random phase approximation, a special case of the general MCLR technique. (*S*)-Oxiranecarbonitrile and the (*R*)-configurations of aziridine-2-carbonitrile are found to be energetically more stable than their mirror images at their equilibrium nuclear configurations. Use of a solvation model to approximate an aqueous environment has a modest, but consistent, effect on the computed parity-violating energies. In the present examples, solvation increases the magnitude of the parity-violating energy by *ca.* 10%.

1. Introduction. – What is the origin of biomolecular homochirality? This nearly exclusive selection of L-amino acids and D-monosaccharides exhibited by terrestrial biochemistry clearly indicates the central role chirality plays in life as we know it. The 'unnatural' counterparts of these biochemical building blocks are not incorporated into proteins and nucleic acids, although they are sometimes found playing very specific biochemical roles. The source of this intriguing biochemical bias can be and has been addressed in a variety of aspects [1–7]. While a *de facto* selection [3][6] can already be understood at the rather basic level of *Fischer*'s 'Lock and Key' hypothesis [8][9], another possibility involves a *de lege* selection [3] due to the parity-violating weak nuclear interaction [2–4][6][10–23]. According to this hypothesis, the very small energy differences between right- and left-handed enantiomers (ΔE_{pv}), which are in the order of 10^{-16} kJ mol^{-1} or a few hundred fJ mol^{-1}, may be decisive for which form (D or L) is selected in real life evolution. Such a question is both subtle and complex, and a definitive answer is hardly impending [6]. However, in a recent theoretical discovery, ΔE_{pv} was found to be frequently more than an order of magnitude larger

[16][17] than previously anticipated, which has sparked renewed interest in the subject [18–28].

To illustrate the physical origin of the aforementioned energy difference (ΔE_{pv}), consider a molecule with a non-superimposable mirror image (*i.e.*, a chiral molecule) such as oxiranecarbonitrile shown in *Fig. 1*.

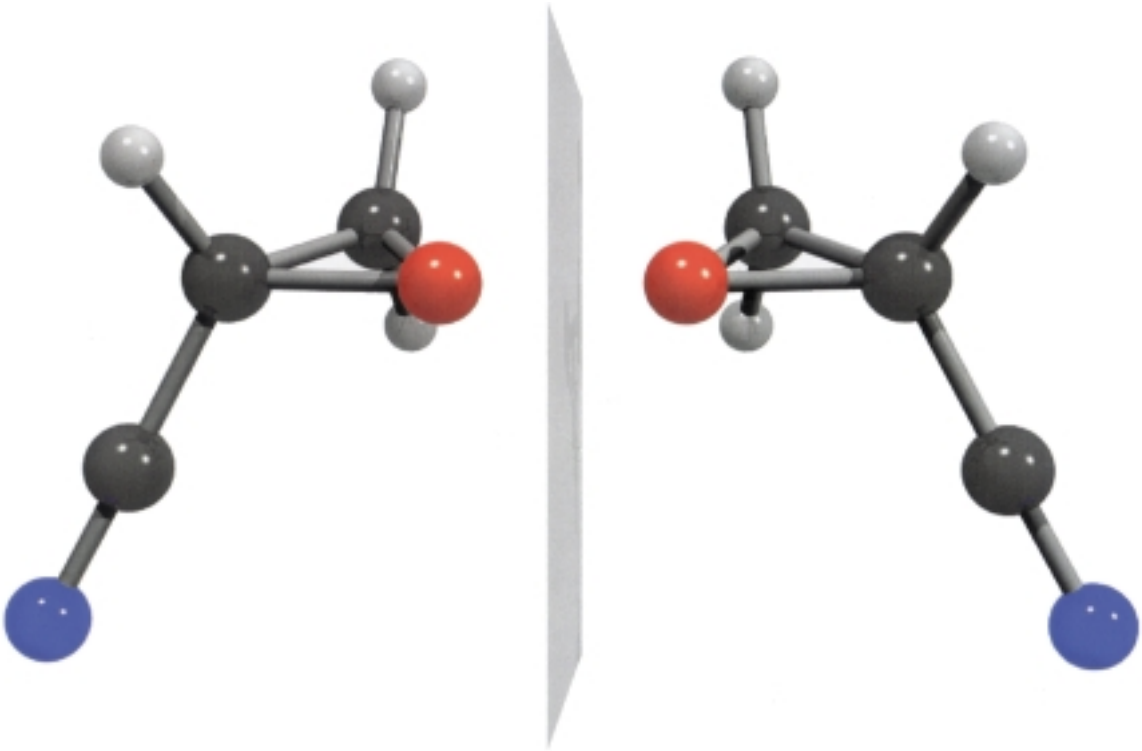

Fig. 1. *The non-superimposable mirror images of chiral oxiranecarbonitrile.* The (*R*)-enantiomer is on the left, and the (*S*)-enantiomer is on the right. C-Atoms are black, H-atoms gray, N-atoms blue, and O-atoms red.

The effective electromagnetic potential experienced by electrons and nuclei in such a molecule free of an external field is said to be parity-conserving, since inverting the spatial coordinates does not change the Hamiltonian (energy) of the system. (This operation is physically equivalent to the mirror reflection typically associated with chemical chirality, since inversion merely involves an additional symmetry operation, namely rotation about an axis perpendicular to the mirror plane, with respect to which all known physical interactions are invariant.) This symmetry results in conservation of the quantum number parity ($+1$ for inversion symmetric states and -1 for antisymmetric states). The eigenstates of the Hamiltonian would have an exact, well-defined parity and would be achiral, as is borne out in conventional quantum-chemical computations, which employ a purely electromagnetic Hamiltonian. While the underlying symmetry is much more general, in the *Born-Oppenheimer* approximation, the computed electronic energies of both enantiomers in *Fig. 1* would be identical.

However, unlike the electromagnetic force, the weak nuclear interaction does not conserve parity. The interaction of electrons and hadrons *via* the weak *neutral* current (mediated by the *chargeless* Z^0 boson) contributes to the effective electronic energy of a molecule. The parity-violating effective potential (E_{pv}) is positive for one enantiomer ($|E_{pv}|$) of a chiral molecule and exactly the negative of this value for its mirror image ($-|E_{pv}|$). In the high barrier limit, which is a realistic approximation for most real chiral molecules having high tunneling barriers for stereomutation, an immediate consequence of electroweak theory is that eigenstates of the Hamiltonians for enantiomers of chiral molecules have different energies and are separated by a total parity-violating energy difference of absolute magnitude

$$|\Delta E_{pv}| = |E_{pv}(\text{left}) - E_{pv}(\text{right})| = 2 \times |E_{pv}| . \quad (1)$$

For a more thorough review of parity violation in atoms and molecules, readers are directed to [3][6][17][29].

The possible role played by parity violation in the homochiral selection of biomolecules can be approached along several different 'molecular' lines of thinking. The first path would be to consider the relative thermodynamic stability of the biochemical building blocks presently found *in vivo*. This track has been the most frequently applied, in fact practically exclusive, approach until today, and might be of consequence if certain relevant steps in kinetic selection schemes [30] are thermodynamically controlled. A second, perhaps more natural, approach may be to consider transition states and rate constants in the same selection schemes. Finally, as yet another route, one can ponder possible biochemical precursor molecules in several contexts, including the abiotic selection of homochirality [31][32].

Previous theoretical studies of parity-violating effects in biomolecules have almost exclusively been directed toward species presently found *in vivo*. However, it may be meaningful to address the question of the relative stability of possible prebiotic precursors of these naturally occurring molecules. Aziridine-2-carbonitrile ($CH_2NHCHCN$) and oxiranecarbonitrile (CH_2OCHCN), also commonly referred to as 2-cyanoaziridine and cyanooxirane, respectively, have been selected as two such potential precursors. In this issue of *Helvetica Chimica Acta* dedicated to *Albert Eschenmoser*, it may be noted that his laboratory was the first to propose these two species as potential precursor molecules during ongoing research that has been referred to as '*an extensive study towards a prebiotic rationalization of the nucleic acid structure*' [33]. An early overview of this work can be found in [34]. The backbone of RNA and of potential precursors such as p-RNA is formed by sugar phosphates. These sugars are readily synthesized *via* aldomerization of glycolaldehyde phosphate [35] under rather naturally occurring conditions [36]. It was in their search for prebiotic pathways to glycolaldehyde phosphate that *Eschenmoser* and co-workers first introduced oxirane-carbonitrile and aziridine-2-carbonitrile in this context. The beginning can be traced back to the first contribution [37] to a series of papers dedicated to understanding the chemistry of α-aminonitriles. The original work focused on 2-aminopropenenitrile, a noncyclic photoisomer of aziridine-2-carbonitrile. The next two installments in the series reported that 2-aminopropenenitrile was indeed convertible to glycolaldehyde phosphate but only *via* photoisomerization to aziridine-2-carbonitrile [38] followed by

a reaction with inorganic phosphate under acidic conditions [39]. *Eschenmoser* and co-workers later proposed isoelectronic oxiranecarbonitrile as a more appealing precursor, since it produced glycolaldehyde phosphate more efficiently and under neutral or basic conditions rather than the harsh acidic conditions required for aziridine-2-carbonitrile [40]. This result prompted the experimental characterization of oxiranecarbonitrile by microwave spectroscopy [41] and a subsequent search for the molecule in interstellar molecular clouds [33]. Although not detected, the extra-terrestrial origin of oxiranecarbonitrile cannot be ruled out, since it is quite possible that it may exist in the heterogeneous environment of interstellar grains and in comets. Regardless of its origin, the prebiotic relevance of oxiranecarbonitrile is still considered an open question by many in the field [42–44]. Although aziridine-2-carbonitrile is less likely to have such relevance, it is included in this study for comparison and completeness. Of course, in general terms, nitriles can also be considered to be precursors of organic acids, including amino acids. Also, aziridine-2-carbonitrile should be seen in the general chemical context of the coupled $CH_4/NH_3/HCN$ system that might be of relevance under conditions in space and planetary atmospheres or in 'soups' as it is in industrial processes [45].

Both oxiranecarbonitrile (*CAS* Reg. No. 4538-51-6) and aziridine-2-carbonitrile (*CAS* Reg. No. 33898-53-2) are chiral molecules existing as a pair of enantiomers. The (*S*)-configuration of the former is displayed in *Fig. 2*,*a*. For the latter, however, the situation is a bit more complex since other low-energy isomers exist. The H-atom bonded to the N-atom in the ring can be on the same or opposite side of the ring plane as the CN group. As shown in *Fig. 2*,*b* and *d*, this situation gives rise to *cis*-aziridine-2-carbonitrile when these two groups are on the same side of the ring and to *trans*-aziridine-2-carbonitrile when they are on opposite sides of this reference plane. The pathway connecting the two diastereoisomers contains a transition structure in which the aforementioned H-atom lies nearly in the plane of the ring, as can be seen in *Fig. 2*,*c*.

This study characterizes these three chiral molecules and one chiral transition structure by conventional (*i.e.*, parity-conserving non-electroweak) *ab initio* electronic-structure techniques. After obtaining a satisfactory description of the electronic properties of these four stationary points, the linear-response approach to electroweak quantum chemistry recently developed in our group was employed to compute the parity-violating energy (E_{pv}) of, and energy separation between (ΔE_{pv}) the (*R*)- and (*S*)-configurations of each pair of enantiomers. These values have also been determined after placing the molecules in a spherical solvent cavity designed as a simple model of an aqueous environment. The present work represents, to our knowledge, the most sophisticated theoretical characterization of these molecules and the first computation of the relative stabilities of the enantiomers of potential prebiotic precursors either in the gas-phase or in an aqueous environment.

2. Theory. – 2.1. *Multi-Configuration Linear-Response Approach to Electroweak Quantum Chemistry.* This section provides some cardinal concepts associated with computing parity-violating energies *via* linear-response techniques. Details of the implementation of this approach are contained in [23]. The parity-violating Hamil-

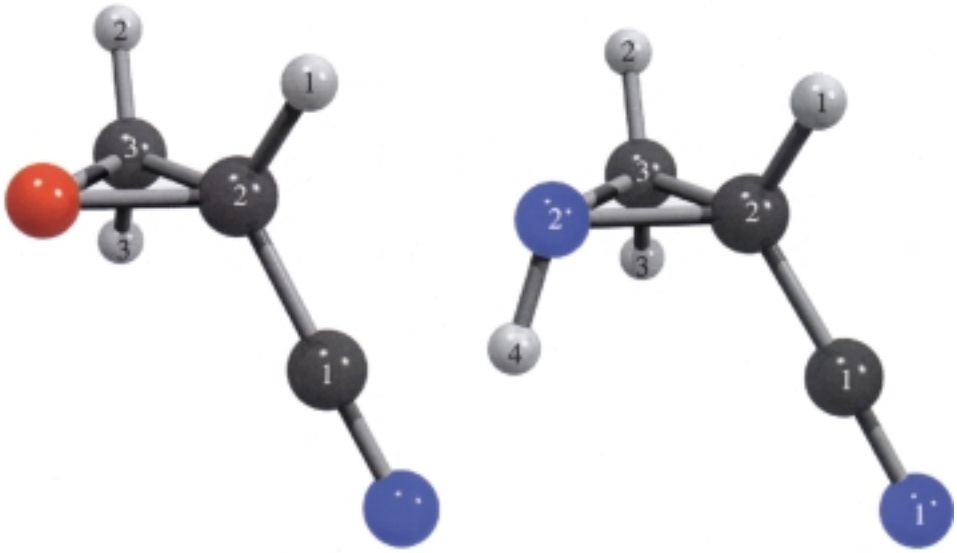

a) CH_2OCHCN

b) *cis*-$CH_2NHCHCN$

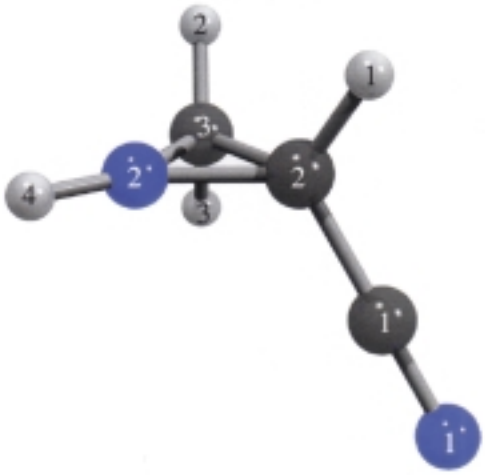

c) $CH_2NHCHCN$ Transition structure

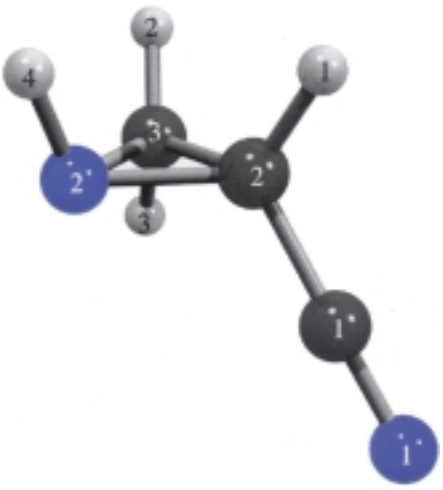

d) *trans*-$CH_2NHCHCN$

Fig. 2. *(*S*)-Configuration of oxiranecarbonitrile and the (*R*)-configurations of aziridine-2-carbonitrile.* The C-atoms are black, H-atoms are gray, N-atoms are blue, and the O-atom is red. Numbers have been included to distinguish between atoms of the same type.

tonian utilized in non-relativistic approaches to electroweak quantum chemistry is dominated by an expression that sums over all electrons (n) and nuclei (N).

$$\hat{H}_{\mathrm{pv}} \approx \frac{G_{\mathrm{F}}\alpha}{2\sqrt{2}} \sum_{i=1}^{n} \sum_{A=1}^{N} Q_{\mathrm{W}}(A) \{\hat{\vec{p}}_i \cdot \hat{\vec{s}}_i, \delta^3(\vec{r}_i - \vec{r}_A)\}_+ \tag{2}$$

Although the actual parity-violating Hamiltonian, $\hat{H}_{\mathrm{pv}}$, is more complex, Eq. 2 illustrates the main features of $\hat{H}_{\mathrm{pv}}$. The prefactor, which includes the *Fermi* constant ($G_{\mathrm{F}} = 2.22254 \times 10^{-14}\ E_{\mathrm{h}}$) and the fine-structure constant (α), is on the order of 10^{-16} E_{h}. (The atomic unit of energy, E_{h}, corresponds to 2625.500 kJ mol^{-1} or 27.2114 eV or 219474.63 cm^{-1}.) Each term in the second sum is proportional to the electroweak charge [$Q_{\mathrm{W}}(A)$] of nucleus A and involves the inner product of the linear momentum ($\hat{p}_i$) and spin ($\hat{s}_i$) operators for the i-th electron. δ^3 is the three-dimensional *Dirac* delta distribution since the short-range weak nuclear force is essentially a contact interaction, and $\{\ldots\}_+$ is the familiar anti-commutator. The electroweak charge (Q_{W}) is given by

$$Q_{\mathrm{W}}(A) = Z_A\ (1 - 4\sin^2(\theta_{\mathrm{W}})) - N_A \tag{3}$$

where Z_A and N_A are the number of protons and neutrons, respectively, in the A-th nucleus. θ_{W} is the experimental value of the *Weinberg* angle used in the present computations ($\sin^2\theta_{\mathrm{W}} = 0.2319$).

The expectation value of $\hat{H}_{\mathrm{pv}}$ for a non-degenerate, pure-spin wave function obtained by typical non-relativistic *ab initio* computations, is exactly zero. Methods like SDE-RHF (single determinant excitation restricted *Hartree-Fock*) [13] and CIS-RHF (configuration interaction single excitation-RHF) [16][17] provide non-vanishing parity-violating potentials by introducing spin-orbit (SO) corrections to the wave function *via* perturbation theory. This approach results in the rather transparent sum-over-states expression for effective parity-violating potential, $E_{\mathrm{pv}}(\vec{r})$, calculated for a specific *Born-Oppenheimer* nuclear configuration, ($\vec{r}$).

$$E_{\mathrm{pv}} = 2\,\mathrm{Re}\left(\sum_j \frac{\langle \Psi_0 \,|\, \hat{H}_{\mathrm{pv}} | \Psi_j \rangle \langle \Psi_j | \hat{H}_{\mathrm{SO}} | \Psi_0 \rangle}{E_0 - E_j} \right) \tag{4}$$

Ψ_0 is usually the singlet, electronic ground-state wave function, and the Ψ_j are excited state, triplet wave functions with corresponding energies E_0 and E_j. $\hat{H}_{\mathrm{SO}}$ is the full *Breit-Pauli* SO operator which includes two-electron terms.

$$\hat{H}_{\mathrm{SO}} = \frac{\alpha^2}{2} \sum_{i=1}^{n} \sum_{A=1}^{N} Z_A \frac{\hat{\vec{l}}_{i,A} \cdot \hat{\vec{s}}_i}{|\vec{r}_A - \vec{r}_i|^3} + \sum_{i=1}^{n} \sum_{i \neq j}^{n} \frac{\hat{\vec{l}}_{i,j} (\hat{\vec{s}}_i + 2\hat{\vec{s}}_j)}{|\vec{r}_i - \vec{r}_j|^3} \tag{5}$$

$\hat{\vec{l}}_{i,\mu}$ is the orbital angular momentum of electron i with respect to the position of particle μ ($\vec{r}_\mu$).

Such a sum-over-states *ansatz* has two major drawbacks. First, the summation converges very slowly with respect to the number of excited states. Second, one is usually restricted to a fairly crude description of the reference state. The recently developed multi-configuration linear-response (MCLR) approach to electroweak

quantum chemistry [23] circumvents both of these dilemmas. The parity-violating potential is given by the linear-response function for a static ($\omega_1 = 0$) perturbation:

$$E_{pv} = \langle\langle \hat{H}_{SO}; \hat{H}_{pv} \rangle\rangle_{\omega_1=0} = \langle\langle \hat{H}_{pv}; \hat{H}_{SO} \rangle\rangle_{\omega_1=0} \quad (6)$$

The MCLR method for computing parity-violating potentials provides improved descriptions of the reference states and at the same time avoids the slow convergence plaguing methods based on a sum-over-states expansion. Systematic investigations of the parity-violating potentials of HOOH show that the random phase approximation (RPA), which is a special case of the more general MCLR approach, can approximately reproduce E_{pv} values from high-level configuration interaction (CI) and complete active space self-consistent field (CASSCF) computations for cases dominated by a single reference state [23].

2.2. *Computational Details.* The nuclear configuration of each stationary point has been optimized using analytic gradient techniques available in the *Gaussian 94* quantum-chemistry package [46] for the restricted *Hartree-Fock* method (RHF) and second-order *Møller-Plesset* perturbation theory (MP2). The residual Cartesian gradients of the equilibrium structures were less than $2 \times 10^{-6}\ E_h\ a_0^{-1}$ (with the *Bohr* radius $a_0 = 52.92$ pm). Each structure has been confirmed as a minimum or transition structure by computing RHF and MP2 analytic second derivatives, from which harmonic vibrational spectra were obtained. The intrinsic reaction coordinate (IRC) of the transition structure was followed in both the forward and reverse directions to ensure that it connects the appropriate minima. During all correlated computations, the five lowest core orbitals were frozen, and five highest virtual orbitals were deleted. All electronic energies were converged to at least $10^{-9}\ E_h$.

As in essentially all conventional molecular-orbital techniques, the wave function is expanded in a set of atomic Gaussian basis functions. For this study, four basis sets of double- and triple-ζ quality with various polarization and higher angular momentum functions were selected. They are denoted DZP, TZP, TZ2P, and TZ2P(*f*,*d*). The smallest basis set, DZP, is constructed by adding one set of polarization functions to the *Huzinaga-Dunning* [47][48] set of contracted double-ζ Gaussian functions with orbital exponents $\alpha_p(H) = 0.75$, $\alpha_d(C) = 0.75$, $\alpha_d(N) = 0.80$, and $\alpha_d(O) = 0.85$. At the core of the remaining basis sets lies *Dunning*'s triple-ζ contraction [49] of *Huzinga*'s primitive Gaussian functions [50]. The TZP basis then augments this contraction with the same single set of polarization functions employed in the DZP basis. The TZ2P basis instead uses two sets of polarization functions with orbital exponents $\alpha_p(H) = 1.5$ and 0.375, $\alpha_d(C) = 1.5$ and 0.375, $\alpha_d(N) = 1.6$ and 0.4, and $\alpha_d(O) = 1.7$ and 0.425. Finally, the TZ2P(*f*,*d*) basis is constructed by adding one set of higher angular momentum functions to the TZ2P basis. The *d*-like functions added to H have orbital exponents of $\alpha_d(H) = 1.0$, while the *f*-like functions added to C, O, and N are $\alpha_f(C) = 0.8$, $\alpha_f(N) = 1.0$, and $\alpha_f(O) = 1.4$, respectively. The final contraction schemes and total number of basis functions for CH_2OCHCN and $CH_2NHCHCN$ are summarized in *Table 1*.

The parity-violating potential (E_{pv}) was computed within the random phase approximation (RPA) for all minima and transition structures by a modified version [23] of the Dalton program [51], which contains the multi-configuration linear-response approach to electroweak quantum chemistry. These computations were

Table 1. *A Description of the Basis Sets Used in this Study.* The last two columns list the total number of basis functions for CH_2OCHCN and $CH_2NHCHCN$, respectively.

Basis sets	C, N, O Contractions	H Contraction	Number of B.F.	
DZP	(9*s*5*p*1*d*/4*s*2*p*1*d*)	(4*s*1*p*/2*s*1*p*)	90	95
TZP	(10*s*6*p*1*d*/5*s*3*p*1*d*)	(5*s*1*p*/3*s*1*p*)	113	119
TZ2P	(10*s*6*p*2*d*/5*s*3*p*2*d*)	(5*s*2*p*/3*s*2*p*)	147	156
TZ2P(*f*,*d*)	(10*s*6*p*2*d*1*f*/5*s*3*p*2*d*1*f*)	(5*s*2*p*1*d*/3*s*2*p*1*d*)	197	211

limited to the DZP, TZP, and TZ2P basis sets due to technical difficulties associated with the storage of a large number of two-electron spin-orbit integrals. Work is currently underway to remove this bottleneck. Use of the RPA was validated by examining the CI coefficients from a CISD computation (CI including all single and double excitations) using the PSI suite of *ab initio* programs [52]. The second most important configuration of each MP2 equilibrium structure has a coefficient with an absolute value of less than 0.03 when employing the TZ2P basis. Clearly, a single reference state dominates the electronic structure of these compounds.

To gain some preliminary insight into the effect that an aqueous environment might exert upon the parity-violating energy difference, a multiconfigurational self-consistent reaction-field (MCSCRF) solvation model was also utilized [25]. The RPA computations were repeated with a simple spherical cavity solvation model available in Dalton using the dielectric constant of H_2O (78.54) at 298 K [53]. The radius of the cavity was set to the maximum distance of an atom (including the *van der Waals* radius) from the molecular center of mass. The numerical values depend upon the molecule considered and are given in the caption of *Fig. 6*. Spherical polynomials through 12th order were used in the evaluation of the one-electron integrals for the solvent calculations.

3. Results and Discussion. – 3.1. *Equilibrium Structures.* The structures of oxiranecarbonitrile and aziridine-2-carbonitrile are depicted in *Fig. 2*. Although different relative configurations of the oxirane and aziridine derivatives are shown (the (*R*)-stereoisomers of aziridine-2-carbonitrile and the (*S*)-stereoisomer of oxiranecarbonitrile), the structures actually have comparable absolute configurations. The presence of the O-atom changes the relative *Cahn-Ingold-Prelog* priority [54] of the CN group. Numbers have been included to distinguish atoms of the same element in order to define the optimized geometrical parameters listed in *Table 2*.

With the exception of the inter-atomic distances within the three-membered rings, all geometrical parameters obtained with the TZ2P and TZ2P(*f*,*d*) basis sets are nearly identical. While more flexible basis sets in conjunction with more sophisticated treatments of both dynamical and static electron correlation are required to achieve similar precision for the highly strained ring, all other bond lengths and angles appear to converge quickly with respect to the number of polarization and higher angular momentum functions for the small group of basis sets employed here. For the purposes of this study, the accuracy obtained with these basis sets is sufficient, as will be evident from results presented in *Sect. 3.4*. As such, only the geometrical parameters obtained from the highest theoretical level [MP2/TZ2P(*f*,*d*)] are reported in *Table 2*. However, to assist future *ab initio* studies of these species, the nuclear Cartesian coordinates of each optimized structure are reported in the *Appendix* accompanying this manuscript.

Table 2. *Select Geometrical Parameters of the Optimized Oxiranecarbonitrile (CH_2OCHCN) and Aziridine-2-carbonitrile ($CH_2NHCHCN$) Structures Obtained at the MP2/TZ2P(*f,d*) Level*. Bond lengths (r_{XY}) are in Å, while bond angles (θ_{XYZ}), torsional angles (τ_{WXYZ}), and angles out of the plane defined by the XC(2)C(3) ring (ϕ_X) are given in degrees. Atom numbers correspond to those found in *Fig. 2*. For certain parameters involving the O- or N-atoms in the ring, X refers to N(2) for aziridine-2-carbonitrile and O for oxiranecarbonitrile. Redundant parameters have been included to facilitate reproduction of Z-matrices.

Parameter	Oxiranecarbonitrile	Aziridine-2-carbonitrile		
		cis	TS	*trans*
$r_{N(1)C(1)}$	1.170	1.171	1.171	1.170
$r_{C(1)C(2)}$	1.445	1.438	1.453	1.440
$r_{XC(2)}$	1.432	1.478	1.397	1.477
$r_{XC(3)}$	1.433	1.468	1.400	1.467
$r_{C(2)C(3)}$	1.468	1.487	1.532	1.486
$r_{H(1)C(2)}$	1.080	1.078	1.084	1.079
$r_{H(2)C(3)}$	1.080	1.078	1.085	1.079
$r_{H(3)C(3)}$	1.080	1.079	1.084	1.078
$r_{H(4)N(2)}$	–	1.015	0.996	1.014
$\theta_{N(1)C(1)C(2)}$	179.1	178.5	179.5	178.6
$\theta_{C(1)C(2)X}$	115.9	118.6	119.3	115.7
$\theta_{C(2)XC(3)}$	61.6	60.6	66.5	60.6
$\theta_{H(1)C(2)X}$	115.1	114.3	119.7	118.4
$\theta_{H(2)C(3)X}$	115.2	114.7	119.2	119.1
$\theta_{H(3)C(3)X}$	115.0	118.7	119.0	114.3
$\theta_{H(4)N(2)C(2)}$	–	108.6	145.0	108.2
$\tau_{C(1)C(2)XC(3)}$	−110.6	−107.3	−106.1	−111.4
$\tau_{H(1)C(2)XC(3)}$	110.7	111.2	105.4	106.7
$\tau_{H(2)C(3)XC(2)}$	−109.4	−109.6	−104.2	−105.9
$\tau_{H(3)C(3)XC(2)}$	109.7	106.3	104.7	110.1
$\tau_{H(4)N(2)C(2)C(3)}$	–	102.2	−179.2	−103.0
$\phi_{C(1)}$	−56.4	−54.7	−52.7	−56.7
$\phi_{H(1)}$	56.7	57.2	52.3	54.7
$\phi_{H(2)}$	54.1	54.7	54.1	56.4
$\phi_{H(3)}$	−53.9	−56.2	−53.9	−54.4
$\phi_{H(4)}$	–	−58.4	0.7	58.1

The total electronic energy (E_{total}), dipole moment (μ_e) and rotational constants (A_e, B_e, C_e) for all optimized structures can be found in *Table 3*. Also included are total energies that include an unscaled, harmonic zero-point vibrational energy contribution (E_{+ZPVE}).

Rotational constants in the vibrational ground state have been determined experimentally from microwave spectroscopy for oxiranecarbonitrile [41] and *cis*-aziridine-2-carbonitrile [55]. The rotational constants were found to be $A_0 = 0.6156\ cm^{-1}$, $B_0 = 0.1176\ cm^{-1}$, and $C_0 = 0.1123\ cm^{-1}$ for the former, and $A_0 = 0.5630\ cm^{-1}$, $B_0 = 0.1177\ cm^{-1}$, and $C_0 = 0.1125\ cm^{-1}$ for the latter. As can been seen in *Table 3*, the computed MP2/TZ2P(*f,d*) rotational constants (A_e, B_e, and C_e) agree well with the experimental values (A_0, B_0, and C_0). Deviations are less than $0.002\ cm^{-1}$, which is of the magnitude expected by just taking the vibrational corrections into account. Although searched for, *trans*-aziridine-2-carbonitrile was not observed in the room-temperature microwave experiment [55].

Table 3. *Energies and Select Properties of the Optimized Oxiranecarbonitrile (CH_2OCHCN) and Aziridine-2-carbonitrile ($CH_2NHCHCN$) Structures.* The total electronic energy (E_{total}) is given in E_h as are the harmonic zero-point corrected energies (E_{+ZPVE}). Dipole moments (μ_e) are in Debye, and rotational constants (A_e, B_e, and C_e) are in cm^{-1}.

	RHF				MP2			
Parameter	DZP	TZP	TZ2P	TZ2P(*f*,*d*)	DZP	TZP	TZ2P	TZ2P(*f*,*d*)
Oxiranecarbonitrile								
E_{total}	−244.64240	−244.67403	−244.68056	−244.69105	−245.35668	−245.44023	−245.49486	−245.57521
E_{+ZPVE}	−244.58135	−244.61322	−244.61980	−244.63021	−245.30032	−245.38394	−245.43895	−245.51889
μ_e	4.085	4.108	4.096	4.083	4.224	4.225	4.208	4.187
A_e	0.640	0.644	0.645	0.647	0.605	0.609	0.609	0.615
B_e	0.118	0.119	0.119	0.119	0.115	0.117	0.117	0.117
C_e	0.113	0.114	0.114	0.114	0.110	0.111	0.112	0.112
cis-Aziridine-2-carbonitrile								
E_{total}	−224.81279	−224.84084	−224.84904	−224.85770	−225.51998	−225.59338	−225.64461	−225.72109
E_{+ZPVE}	−224.73799	−224.76639	−224.77446	−224.78321	−225.45034	−225.52404	−225.57548	−225.65176
μ_e	2.963	3.024	3.090	3.084	3.059	3.098	3.161	3.145
A_e	0.580	0.584	0.584	0.586	0.558	0.563	0.562	0.565
B_e	0.118	0.119	0.119	0.119	0.115	0.117	0.117	0.118
C_e	0.113	0.114	0.114	0.114	0.110	0.112	0.112	0.113
cis/*trans*-Aziridine-2-carbonitrile transition structure								
E_{total}	−224.78389	−224.81294	−224.81968	−224.83008	−225.48799	−225.56366	−225.61365	−225.69136
E_{+ZPVE}	−224.71150	−224.74080	−224.74748	−244.75791	−225.42040	−225.49621	−225.54643	−225.62395
μ_e	4.336	4.367	4.402	4.392	4.458	4.457	4.490	4.477
A_e	0.594	0.599	0.600	0.601	0.575	0.582	0.581	0.585
B_e	0.116	0.117	0.117	0.117	0.113	0.115	0.115	0.116
C_e	0.110	0.111	0.111	0.111	0.108	0.109	0.110	0.110
trans-Aziridine-2-carbonitrile								
E_{total}	−224.81195	−224.84021	−224.84820	−224.85691	−225.51841	−225.59231	−225.64320	−225.71959
E_{+ZPVE}	−224.73720	−224.76581	−224.77369	−224.78249	−225.44890	−225.52304	−225.57414	−225.65035
μ_e	5.330	5.359	5.299	5.288	5.459	5.466	5.403	5.394
A_e	0.602	0.606	0.606	0.608	0.576	0.582	0.581	0.585
B_e	0.116	0.117	0.117	0.117	0.113	0.115	0.115	0.116
C_e	0.110	0.111	0.111	0.111	0.108	0.109	0.109	0.110

Also reported in the experimental characterization of oxiranecarbonitrile was an electric dipole moment (μ_0) of 3.740 D. At the MP2/TZ2P(*f*,*d*) level, a value for μ_e of 4.187 D has been computed. Although the discrepancy between theory and experiment appears to be large, one must keep in mind that μ_e and μ_0 are two different quantities and should not be directly compared without correcting one or both quantities. On the theoretical side, the lack of adequate diffuse functions may introduce some 10% error in μ_e.

3.2. *Harmonic Vibrational Spectra.* The harmonic vibrational wavenumbers of each species obtained at the MP2 theoretical level are presented in *Tables 4–7.* Also included are the corresponding infrared (IR) band strengths determined within the double harmonic approximation. Data from the RHF computations are included in the *Appendix* to assist those who wish to introduce non-uniform scaling in an attempt to construct a more sophisticated approximation of the zero-point vibrational energy than that used here (*vida infra*). Band strengths, which have dimensions of a cross section (pm^2), are reported rather than the commonly utilized IR intensities, which have dimensions of length (km or km mol^{-1}). The rationale behind

this choice is described in detail in [56–58], as are the derivations of the conversion between band strengths and other common units for reporting IR intensity. Presently, the relation

$$G/\mathrm{pm}^2 \approx 16.60540 \frac{(\overline{A}/\mathrm{km\,mol}^{-1})}{(\omega_e/\mathrm{cm}^{-1})} \tag{7}$$

has been used to convert the IR intensity from km mol^{-1} ($\overline{A}$) to pm^2 (G). The operational definitions are

$$G \equiv \int \sigma(\tilde{\nu})\tilde{\nu}^{-1}\mathrm{d}\tilde{\nu} \approx \tilde{\nu}_0^{-1} \int \sigma(\tilde{\nu})\mathrm{d}\tilde{\nu} = \frac{\overline{A}}{\tilde{\nu}_0 N_A} \tag{8}$$

where N_A is the *Avogadro*'s constant. Most quantum-chemical program packages actually compute the transition dipole moment in the vibrationally harmonic-linear dipole-function approximation, with $G_{\mathrm{theoretical}}$ being then proportional to the absolute square of the transition dipole matrix element [58].

$$G_{\mathrm{theroetical}} = \frac{8\pi^3}{(4\pi\varepsilon_0)3hc} |\langle \nu_f = 1|\,\mu|\nu_i = 0\rangle|^2 \tag{9}$$

The *Tables 4–7* show that convergence of the vibrational frequencies mimics that observed for the optimized geometrical parameters. Only modes that mix heavily with the ring stretching vibrations exhibit variations larger than a few cm^{-1} between the two largest basis sets employed.

Table 4. Ab initio *Harmonic Vibrational Spectrum of Oxiranecarbonitrile (CH_2OCHCN) Obtained at the MP2 Level of Theory*. The unscaled harmonic wavenumbers (ω) are in cm^{-1} while the corresponding double harmonic band strengths (G) are in pm^2.

Mode	DZP		TZP		TZ2P		TZ2P(*f*,*d*)	
	ω/cm^{-1}	G/pm^2	ω/cm^{-1}	G/pm^2	ω/cm^{-1}	G/pm^2	ω/cm^{-1}	G/pm^2
ν_1	3301	0.045	3268	0.037	3278	0.025	3279	0.024
ν_2	3233	0.024	3209	0.013	3221	0.011	3222	0.010
ν_3	3182	0.081	3158	0.055	3171	0.053	3170	0.050
ν_4	2167	0.038	2193	0.037	2180	0.028	2200	0.024
ν_5	1553	0.017	1544	0.014	1529	0.009	1531	0.011
ν_6	1421	0.135	1415	0.115	1396	0.105	1412	0.110
ν_7	1286	0.083	1287	0.093	1264	0.111	1282	0.112
ν_8	1170	0.020	1185	0.008	1168	0.005	1175	0.002
ν_9	1168	0.004	1174	0.025	1155	0.029	1164	0.033
ν_{10}	1098	0.073	1106	0.059	1095	0.075	1105	0.061
ν_{11}	1060	0.119	1065	0.114	1052	0.104	1058	0.114
ν_{12}	945	0.770	938	0.695	912	0.612	938	0.677
ν_{13}	873	0.399	864	0.431	838	0.466	867	0.374
ν_{14}	795	0.222	793	0.228	779	0.218	795	0.214
ν_{15}	547	0.079	549	0.081	550	0.101	558	0.092
ν_{16}	521	0.038	529	0.040	527	0.018	532	0.020
ν_{17}	214	0.578	219	0.596	218	0.617	222	0.608
ν_{18}	205	0.302	213	0.341	208	0.386	211	0.379

Table 5. Ab initio *Vibrational Spectrum of* cis-*Aziridine-2-carbonitrile ($CH_2NHCHCN$) Obtained at the MP2 Level of Theory.* The unscaled harmonic wavenumbers (ω) are in cm^{-1}, while the corresponding double harmonic band strengths (G) are in pm^2.

Mode	DZP		TZP		TZ2P		TZ2P(*f*,*d*)	
	ω/cm^{-1}	G/pm^2	ω/cm^{-1}	G/pm^2	ω/cm^{-1}	G/pm^2	ω/cm^{-1}	G/pm^2
ν_1	3566	0.031	3518	0.038	3544	0.051	3538	0.059
ν_2	3314	0.024	3280	0.022	3290	0.014	3290	0.013
ν_3	3253	0.008	3228	0.004	3241	0.003	3239	0.003
ν_4	3199	0.051	3174	0.038	3188	0.035	3184	0.032
ν_5	2164	0.008	2189	0.008	2175	0.010	2195	0.014
ν_6	1541	0.014	1534	0.014	1520	0.015	1518	0.016
ν_7	1408	0.054	1400	0.046	1386	0.048	1396	0.038
ν_8	1305	0.095	1298	0.065	1299	0.118	1300	0.086
ν_9	1264	0.147	1263	0.146	1251	0.158	1252	0.145
ν_{10}	1200	0.280	1199	0.258	1197	0.279	1195	0.293
ν_{11}	1156	0.060	1166	0.049	1148	0.039	1149	0.042
ν_{12}	1129	0.072	1138	0.065	1118	0.081	1118	0.082
ν_{13}	1031	0.125	1032	0.147	1025	0.200	1025	0.160
ν_{14}	973	0.169	974	0.148	962	0.135	965	0.141
ν_{15}	939	0.463	928	0.408	908	0.385	926	0.421
ν_{16}	856	0.869	831	0.841	819	0.725	839	0.766
ν_{17}	790	0.326	783	0.418	774	0.309	788	0.332
ν_{18}	543	0.082	546	0.056	548	0.032	554	0.033
ν_{19}	522	0.057	527	0.035	528	0.023	534	0.019
ν_{20}	214	0.753	216	0.805	217	0.807	220	0.811
ν_{21}	203	0.725	209	0.812	206	0.852	208	0.848

Table 6. Ab initio *Harmonic Vibrational Spectrum of the Aziridine-2-carbonitrile ($CH_2NHCHCN$) Transition Structure Obtained at the MP2 Level of Theory.* The unscaled harmonic wavenumbers (ω) are in cm^{-1}, while the corresponding double harmonic band strengths (G) are in pm^2.

Mode	DZP		TZP		TZ2P		TZ2P(*f*,*d*)	
	ω/cm^{-1}	G/pm^2	ω/cm^{-1}	G/pm^2	ω/cm^{-1}	G/pm^2	ω/cm^{-1}	G/pm^2
ν_1	3815	0.605	3790	0.572	3794	0.555	3791	0.575
ν_2	3234	0.140	3197	0.136	3213	0.113	3209	0.108
ν_3	3179	0.096	3149	0.091	3167	0.082	3164	0.077
ν_4	3133	0.223	3106	0.218	3123	0.203	3118	0.198
ν_5	2158	0.021	2185	0.017	2172	0.011	2191	0.009
ν_6	1571	0.143	1564	0.120	1554	0.089	1551	0.103
ν_7	1437	0.453	1430	0.427	1412	0.386	1424	0.402
ν_8	1326	0.185	1329	0.243	1309	0.313	1321	0.258
ν_9	1173	0.007	1182	0.000	1172	0.008	1175	0.001
ν_{10}	1160	0.091	1166	0.023	1159	0.052	1157	0.037
ν_{11}	1141	0.234	1142	0.323	1130	0.272	1129	0.263
ν_{12}	1086	0.046	1089	0.050	1073	0.043	1082	0.047
ν_{13}	1053	0.046	1057	0.036	1046	0.053	1049	0.040
ν_{14}	992	0.128	997	0.118	986	0.061	988	0.117
ν_{15}	919	0.312	913	0.299	893	0.245	913	0.264
ν_{16}	794	0.332	793	0.345	784	0.349	795	0.300
ν_{17}	566	0.008	571	0.007	573	0.007	577	0.007
ν_{18}	517	0.054	523	0.049	523	0.047	529	0.046
ν_{19}	212	0.171	217	0.211	217	0.227	221	0.229
ν_{20}	201	0.225	207	0.248	205	0.293	207	0.290
ν_{21}	944*i*	–	917*i*	–	915*i*	–	919*i*	–

Table 7. Ab initio *Harmonic Vibrational Spectrum of* trans-*Aziridine-2-carbonitrile ($CH_2NHCHCN$) Obtained at the MP2 Level of Theory.* The unscaled harmonic wavenumbers (ω) are in cm^{-1}, while the corresponding double harmonic band strengths (G) are in pm^2.

Mode	DZP		TZP		TZ2P		TZ2P(*f*,*d*)	
	ω/cm^{-1}	G/pm^2	ω/cm^{-1}	G/pm^2	ω/cm^{-1}	G/pm^2	ω/cm^{-1}	G/pm^2
ν_1	3570	0.022	3526	0.028	3553	0.041	3547	0.050
ν_2	3312	0.020	3280	0.017	3290	0.010	3290	0.010
ν_3	3239	0.016	3212	0.012	3228	0.008	3227	0.008
ν_4	3196	0.061	3172	0.047	3187	0.042	3183	0.039
ν_5	2173	0.007	2199	0.007	2185	0.004	2204	0.004
ν_6	1543	0.005	1534	0.003	1521	0.003	1520	0.003
ν_7	1436	0.055	1431	0.053	1418	0.058	1426	0.056
ν_8	1293	0.090	1292	0.077	1288	0.154	1284	0.093
ν_9	1250	0.260	1241	0.159	1228	0.320	1236	0.230
ν_{10}	1213	0.234	1212	0.291	1214	0.107	1207	0.235
ν_{11}	1142	0.037	1151	0.029	1133	0.046	1132	0.044
ν_{12}	1121	0.012	1132	0.007	1121	0.008	1121	0.006
ν_{13}	998	0.056	1000	0.085	990	0.104	994	0.048
ν_{14}	955	0.258	958	0.223	942	0.222	945	0.279
ν_{15}	924	0.352	916	0.268	902	0.311	910	0.227
ν_{16}	880	0.836	858	0.897	844	0.680	863	0.847
ν_{17}	794	0.206	792	0.246	781	0.221	792	0.192
ν_{18}	542	0.171	546	0.199	547	0.222	553	0.213
ν_{19}	515	0.059	524	0.072	520	0.043	526	0.053
ν_{20}	215	0.166	219	0.178	218	0.185	222	0.180
ν_{21}	204	0.046	211	0.057	207	0.086	209	0.084

3.3 *Isomerization of Aziridine-2-carbonitrile.* At all levels of theory, *cis*-aziridine-2-carbonitrile is slightly more stable than the *trans*-isomer. Interconversion of the two diastereoisomers can be achieved by flipping the H-atom bonded to the N-atom to the other side of the NCC ring. Such a flipping motion is equivalent to inversion at the N-atom. This isomerization pathway contains an electronic barrier near 80 kJ mol^{-1} as depicted in *Fig. 3*. Since *cis*-aziridine-2-carbonitrile is consistently the most stable species, it forms a convenient reference. Thus, the ΔE_e and $\Delta E_e^{\ddagger}$ shown in *Fig. 3* are the energies of *trans*-aziridine-2-carbonitrile and the transition structure relative to the *cis*-isomer, respectively. Zero-point vibrational energy (ZPVE) corrections have been determined from the unscaled harmonic frequencies. The imaginary frequency was excluded from the ZPVE correction to the energy of the transition structure. The values of ΔE_e and $\Delta E_e^{\ddagger}$ (and their harmonic ZPVE corrected counterparts) are collected in *Table 8*. It should be noted that, although these data are reported to a numerical precision of 0.01 kJ mol^{-1} to facilitate comparison with future studies, the estimated uncertainty of the best computations presented here is on the order of a few kJ mol^{-1}.

At the highest level of theory employed [MP2/TZ2P(*f*,*d*)], ΔE_e is only 3.95 kJ mol^{-1}. Including the ZPVE has almost no effect (-0.24 kJ mol^{-1}). However, the difference between $\Delta E_e^{\ddagger}$ or $\Delta E_0^{\ddagger}$ is significantly larger (5 kJ mol^{-1}). Taking one of the two modes with wavenumbers near 800 cm^{-1} as the reaction coordinate, the primary zero-point effect solely from this mode would be nearly 5 kJ mol^{-1}. One must note, however, that ν_1, for instance, increases substantially in the transition structure as expected for an sp^2-hybridized NH stretching mode. In fact, the ZPVE corrections result from a

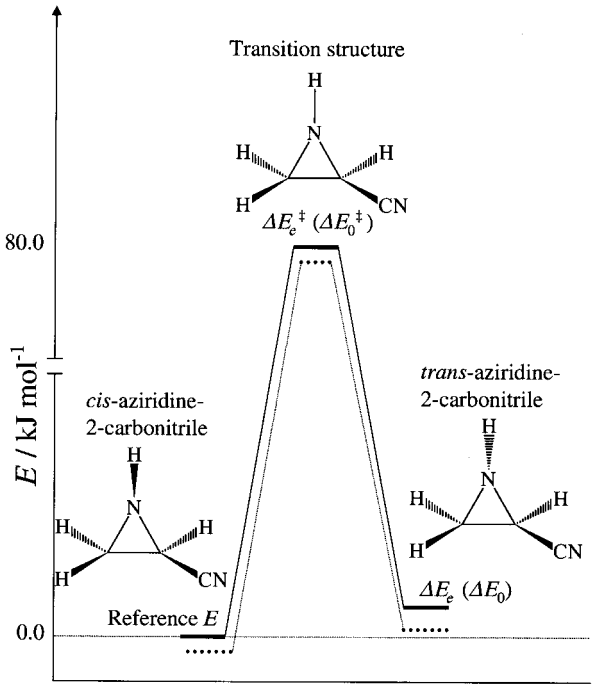

Fig. 3. *A representation of the isomerization pathway between* cis- *and* trans-*aziridine-2-carbonitrile.* For convenience, the energy of *cis*-aziridine-2-carbonitrile is defined as zero. The energies of the transition structure and the *trans*-isomer ($\Delta E_e^{\ddagger}$ and ΔE_e, respectively) are ascertained relative to this reference energy. Energy differences, which include unscaled harmonic zero-point energy corrections, are denoted ΔE_0 and $\Delta E_0^{\ddagger}$. These data are tabulated in *Table 8*. The dotted lines represent the energy shifts due to E_{pv} for the (*R*)-enantiomers of the three species after being scaled by *ca.* 10^{16}. *Table 9* contains the E_{pv} values.

Table 8. *The Energies of* trans-*Aziridine-2-carbonitrile* (ΔE_e) *and the Transition Structure* ($\Delta E_e^{\ddagger}$) *Relative to That of* cis-*Aziridine-2-carbonitrile as Depicted in* Fig. 3. Listed in parentheses are the zero-point corrected values (ΔE_0 and $\Delta E_0^{\ddagger}$). Note that $\Delta E_0^{\ddagger}$ is obtained from unscaled harmonic vibrational frequencies and does not include the imaginary frequency of the transition structure. The tabulated data are listed in kJ mol^{-1}.

Basis	$\Delta E_e^{\ddagger}$	$\Delta E_0^{\ddagger}$	ΔE_e	ΔE_0
	RHF			
DZP	75.89	(69.53)	2.22	(2.06)
TZP	73.27	(67.18)	1.67	(1.51)
TZ2P	77.09	(70.83)	2.19	(2.02)
TZ2P(*f*,*d*)	72.52	(66.41)	2.08	(1.90)
	MP2			
DZP	84.00	(78.61)	4.12	(3.79)
TZP	78.02	(73.08)	2.79	(2.63)
TZ2P	81.29	(76.27)	3.69	(3.52)
TZ2P(*f*,*d*)	78.05	(73.02)	3.95	(3.71)

complicated contribution from all modes. MP2 Computations with the largest basis set predict an electronic isomerization barrier of 78.05 kJ mol^{-1}. The ZPVE correction decreases the value to 73.02 kJ mol^{-1}.

Only one experimental estimate of these energy differences for aziridine-2-carbonitrile has been found in the literature [55]. From the absence of lines from the *trans*-isomer in the room-temperature microwave spectrum of aziridine-2-carbonitrile, it was inferred that the *trans*-diastereoisomer must lie at least 11 kJ mol^{-1} higher in energy than the *cis*-isomer. The results from the present investigation, along with theoretical and experimental determinations of analogous energy separations for similar compounds, suggest that the true energy difference is substantially lower. Our calculations suggest a re-investigation of the isomerization energy, perhaps best by quantitative IR spectroscopy [58] (for instance, in the ν_7 fundamental; such work is planned in our laboratory).

An inversion barrier for aziridine of 79.9 kJ mol^{-1} has been inferred from gas-phase ^{1}H-NMR spectra [59]. In excellent agreement is a theoretical value of 79.4 kJ mol^{-1} from a focal point analysis [60–63] of high quality *ab initio* computations for aziridine [64]. The same theoretical study examined *cis*- and *trans*-2-methylaziridine. MP2 Energies obtained with a fairly prodigious basis set reveal that the analogous transition structure lies 79.83 kJ mol^{-1} above the more stable diastereomer (74.89 kJ mol^{-1} with a scaled harmonic ZPVE correction), which is again very similar to the values obtained in this study. An earlier *ab initio* investigation [63] of protonated, monosubstituted oxirane cations included the analogous CN derivatives of the oxonium ions, which are isoelectronic with aziridine-2-carbonitrile. Their equivalent of ΔE_e lies between 3 and 4 kJ mol^{-1}, and is rather similar to our observations.

It should be noted, however, that the relative stability of *cis*- and *trans*-2-methylaziridine [64] is opposite to that observed here for aziridine-2-carbonitrile (2-cyanoaziridine). The work on various derivatives of protonated oxirane positive ions lends some insight by showing a correlation between the relative stability of the diastereoisomers and the total atomic charge (obtained by a *Mulliken* population analysis [66–68]) of the substituent group [65]. If the group has a significant accumulation of negative charge (F and CN), then the *cis*-isomer is more stable. No or positive charge accumulation on the substituent group (Me, CHO, and CHNH) is found when the *trans*-isomer lies lower in energy. Of course, the situation is far more complex than a purely electrostatic model could describe. Photoelectron spectra and MNDO computations reveal quite different electronic structures for Me- and CN-substituted aziridines [69]. In that work, it is speculated that interaction of a π orbital from the CN group with the ring (and indirectly with the N lone-pair orbital in the ring) constitutes the major source of the qualitative discrepancies. Mentioned here as well are the classic studies of stabilization of chiral aziridines by electronegative (*e.g.*, N–Cl) substitution at the N-atom by *Felix* and *Eschenmoser* [70].

3.4. *Parity-Violating Energy Differences and Potentials. Table 9* contains the values of the parity-violating energy E_{pv} computed within the random phase approximation (RPA) for a variety of optimized nuclear configurations of oxiranecarbonitrile and aziridine-2-carbonitrile. E_{pv} is negative for (*S*)-oxiranecarbonitrile, indicating that this stereoisomer of CH_2OCHCN is more stable than its mirror image by twice the absolute value of E_{pv}. Thus, $|\Delta E_{pv}|$ is nearly 10^{-19} E_h or 200 fJ mol^{-1} for oxiranecarbonitrile. In

contrast, for all three stationary points of aziridine-2-carbonitrile examined, the (*R*)-conformer is more stable than its (*S*)-counterpart, and $|\Delta E_{pv}|$ is *ca.* 4×10^{-20} E_h or 80 fJ mol^{-1}.

Table 9. E_{pv} of *(S)-Oxiranecarbonitrile and (R)-Aziridine-2-carbonitrile.* The data in parentheses were obtained using the solvation model described in the text. Values are in units of 10^{-20} E_h. The first column indicates the level at which the equilibrium structure was obtained.

Optimized structure	Oxiranecarbonitrile		Aziridine-2-carbonitrile					
			cis		TS		*trans*	
RPA with DZP Basis								
RHF/DZP	− 4.05	(− 4.51)	− 1.33	(− 1.43)	− 1.39	(− 1.79)	− 1.76	(− 1.91)
RHF/TZP	− 4.04	(− 4.49)	− 1.37	(− 1.47)	− 1.40	(− 1.80)	− 1.71	(− 1.86)
RHF/TZ2P	− 3.96	(− 4.41)	− 1.29	(− 1.38)	− 1.38	(− 1.77)	− 1.68	(− 1.83)
RHF/TZ2P(*f*,*d*)	− 4.02	(− 4.48)	− 1.32	(− 1.43)	− 1.39	(− 1.79)	− 1.69	(− 1.84)
MP2/DZP	− 4.09	(− 4.60)	− 1.51	(− 1.61)	− 1.31	(− 1.78)	− 1.76	(− 1.91)
MP2/TZP	− 4.04	(− 4.53)	− 1.53	(− 1.62)	− 1.30	(− 1.76)	− 1.70	(− 1.84)
MP2/TZ2P	− 3.88	(− 4.36)	− 1.40	(− 1.48)	− 1.29	(− 1.74)	− 1.63	(− 1.77)
MP2/TZ2P(*f*,*d*)	− 4.06	(− 4.55)	− 1.46	(− 1.54)	− 1.33	(− 1.78)	− 1.69	(− 1.83)
RPA with TZP Basis								
RHF/DZP	− 4.40	(− 4.95)	− 1.51	(− 1.66)	− 1.57	(− 2.04)	− 2.04	(− 2.22)
RHF/TZP	− 4.38	(− 4.92)	− 1.56	(− 1.71)	− 1.59	(− 2.05)	− 1.99	(− 2.17)
RHF/TZ2P	− 4.31	(− 4.84)	− 1.48	(− 1.62)	− 1.57	(− 2.03)	− 1.96	(− 2.13)
RHF/TZ2P(*f*,*d*)	− 4.38	(− 4.91)	− 1.52	(− 1.66)	− 1.58	(− 2.04)	− 1.97	(− 2.15)
MP2/DZP	− 4.37	(− 4.98)	− 1.66	(− 1.80)	− 1.48	(− 2.02)	− 2.06	(− 2.24)
MP2/TZP	− 4.33	(− 4.92)	− 1.69	(− 1.82)	− 1.48	(− 2.01)	− 2.00	(− 2.17)
MP2/TZ2P	− 4.16	(− 4.73)	− 1.55	(− 1.68)	− 1.49	(− 2.00)	− 1.93	(− 2.09)
MP2/TZ2P(*f*,*d*)	− 4.39	(− 4.97)	− 1.63	(− 1.75)	− 1.52	(− 2.04)	− 2.00	(− 2.17)
RPA with TZ2P Basis								
RHF/DZP	− 4.50	(− 5.07)	− 1.54	(− 1.69)	− 1.70	(− 2.18)	− 2.10	(− 2.28)
RHF/TZP	− 4.49	(− 5.04)	− 1.58	(− 1.73)	− 1.72	(− 2.19)	− 2.05	(− 2.22)
RHF/TZ2P	− 4.41	(− 4.96)	− 1.50	(− 1.64)	− 1.70	(− 2.16)	− 2.02	(− 2.19)
RHF/TZ2P(*f*,*d*)	− 4.48	(− 5.03)	− 1.54	(− 1.69)	− 1.71	(− 2.18)	− 2.03	(− 2.21)
MP2/DZP	− 4.48	(− 5.09)	− 1.68	(− 1.83)	− 1.60	(− 2.15)	− 2.10	(− 2.27)
MP2/TZP	− 4.43	(− 5.03)	− 1.70	(− 1.84)	− 1.61	(− 2.14)	− 2.04	(− 2.20)
MP2/TZ2P	− 4.26	(− 4.84)	− 1.56	(− 1.70)	− 1.61	(− 2.13)	− 1.96	(− 2.12)
MP2/TZ2P(*f*,*d*)	− 4.48	(− 5.07)	− 1.63	(− 1.77)	− 1.65	(− 2.17)	− 2.04	(− 2.20)

It is interesting to note that, in these molecules, E_{pv} and ΔE_{pv} are somewhat insensitive to the level at which the geometry optimizations are carried out. Whether the equilibrium structure is obtained with a correlated (MP2) or uncorrelated (RHF) technique, or with a small (DZP) or large [TZ2P(*f*,*d*)] basis set, the parity-violating energy computed for the gas-phase equilibrium structure changes less than 20% on average. This observation has important ramifications since the magnitude of the parity-violating energy is still an open question. In cases like the present one, a highly accurate equilibrium structure is apparently not required to obtain a reasonable estimate of E_{pv}. Of course, E_{pv} is truly a geometry-dependent property [17]. Vibrational- and rotational-frequency shifts due to this dependence of the parity-violating potential upon nuclear configuration have been computed, for instance, as a function of reduced normal coordinates for CHFClBr [71][72], and fluorooxirane [74][75].

Also noteworthy is the fact that the values of $|\Delta E_{pv}|$ slightly but consistently increase as one moves to larger basis sets (DZP → TZP → TZ2P). This effect is illustrated in *Fig. 4* for the set of MP2-optimized gas-phase structures obtained with the TZ2P(*f*,*d*) basis set. The larger initial change between the DZP and TZP bases becomes less pronounced when moving from the TZP basis to the TZ2P set. As basis-set saturation has certainly not been reached, we expect the RPA limit of $|\Delta E_{pv}|$ to be slightly (perhaps *ca.* 40%) larger than the value obtained with the TZ2P basis set.

A similar effect is observed by computing E_{pv} after placing the molecules in a spherical solvent cavity. Again using the MP2/TZ2P(*f*,*d*) optimized structures for illustrating the general trend, *Fig. 5* shows the consistent increase in $|\Delta E_{pv}|$ after solvation. The effect is most pronounced for oxiranecarbonitrile. In all cases, however, the increase is *ca.* 10% of the gas-phase value. Solvation effects of similar magnitude have been found for neutral alanine, while larger effects are observed for the zwitterionic form [25].

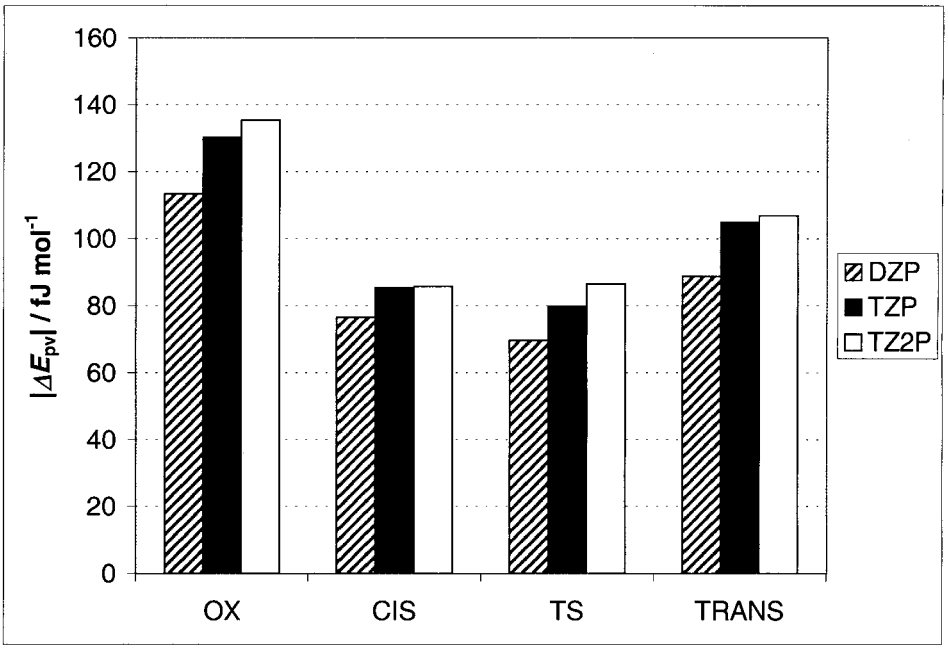

Fig. 4. *The effect of increasing basis-set size on the computed value of* ΔE_{pv} *within the RPA approximation.* All values have been determined using the MP2/TZ2P(*f*,*d*)-optimized nuclear configurations for oxiranecarbonitrile (OX), *cis*-aziridine-2-carbonitrile (CIS), the *cis*/*trans*-transition structure (TS), and *trans*-aziridine-2-carbonitrile (TRANS). The OX values have been decreased by 100 fJ mol^{-1} to facilitate comparison with the aziridine-2-carbonitrile data.

Since the cavity radius of the solvation model employed here has an effect on the computed molecular properties, the radius was systematically varied over a range from 6.5 a_0 to 25.0 a_0 in order to characterize the influence upon the parity-violating energy difference. *Fig. 6* shows the value of $|\Delta E_{pv}|$ as a function of the cavity radius for all four species examined in this study. Although $|\Delta E_{pv}|$ changes significantly with the

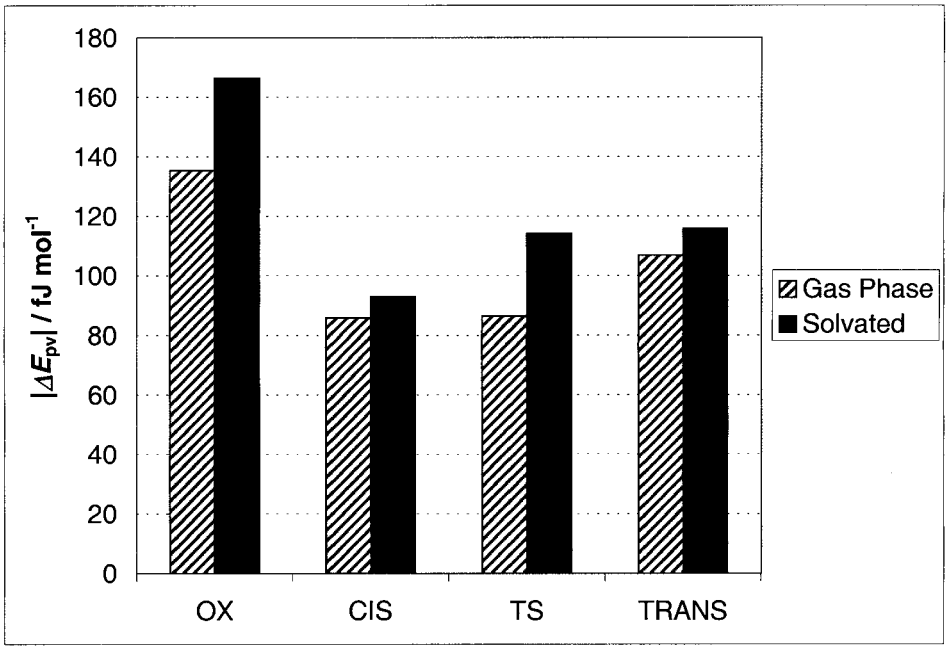

Fig. 5. *The effect of solvation on the computed value of* ΔE_{pv} *within the RPA approximation and employing the DZP basis.* All values have been determined using the MP2/TZ2P(*f*,*d*)-optimized nuclear configurations for oxiranecarbonitrile (OX), *cis*-aziridine-2-carbonitrile (CIS), the *cis*/*trans*-transition structure (TS), and *trans*-aziridine-2-carbonitrile (TRANS). The OX values have been decreased by 100 fJ mol^{-1} to facilitate comparison with the aziridine-2-carbonitrile data (for cavity sizes, see caption of *Fig. 6*).

size of the solvent cavity, it is clear that solvation for any reasonable cavity radius significantly and consistently increases the parity-violating energy difference. Only for unreasonably large radii does the solvation model have a negligible effect.

4. Conclusions. – The present work is the first to study parity violation in possible precursor molecules in biochemical evolution, and as such, has a highly exploratory character. One can be rather confident about the basic quantum-chemical characterization of oxiranecarbonitrile and aziridine-2-carbonitrile. This effort by itself provides useful and new, albeit rather conventional, information about these precursor molecules introduced by *Eschenmoser* and co-workers. Much less conventional are the results on parity-violating energy differences and potentials as summarized in *Table 9* and *Fig. 3*. While this type of result still has the character of frontier research, it seems from recent systematic approaches that, at the very least, the order of magnitude and sign of parity-violating energy differences in chiral molecules can now be specified with a reasonable degree of certainty. This estimate is a major step forward with respect to essentially all calculations of the last two decades, which have to be questioned with respect to both of these points, as has been shown before [16–18][23–25]. As already pointed out, previous claims of preferential stabilization of L-amino acids, in particular, must be rejected for several reasons [16][17][25].

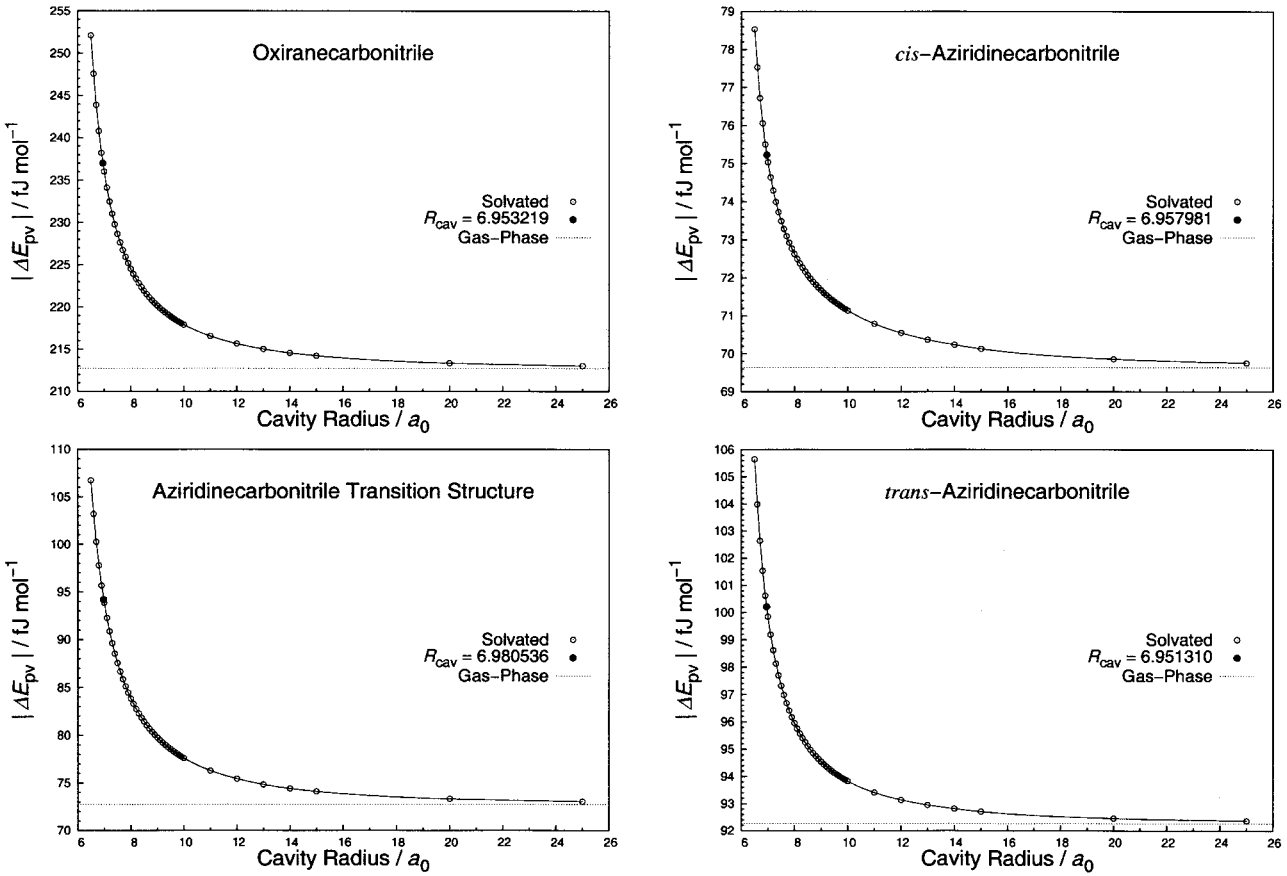

Fig. 6. *Effect of cavity size on the parity-violating energy difference,* $|\Delta E_{pv}|$, *computed at the RPA/DZP level using the RHF/DZP-optimized gas-phase structures.* The open circles represent the computed values of $|\Delta E_{pv}|$ using arbitrary cavity radii ($R_{cav} = 6.5, 6.6, \ldots, 9.9, 10.0, 11.0, \ldots, 14.0, 15.0, 20.0$, and $25.0\ a_0$), while the solid circles in each graph correspond to a cavity radius equal to the maximum distance of an atom including its *van der Waals* radius from the molecular center of mass ($R_{cav} = 6.953219\ a_0$ for oxiranecarbonitrile, $R_{cav} = 6.957981\ a_0$ for *cis*-aziridinecarbonitrile, $R_{cav} = 6.951310\ a_0$ for *trans*-aziridinecarbonitrile, and $R_{cav} = 6.980536\ a_0$ for transition structure). The dotted lines show the value of $|\Delta E_{pv}|$ in the absence of any cavity (*i.e.*, the gas-phase value). Clearly, solvation increases the magnitude of E_{pv} and ΔE_{pv} for any reasonably chosen cavity size. See also text for details.

In terms of the enthalpy of reaction at zero K ($\Delta_R H_0^0$) for the enantiomerization reactions, one can consider the following in the context of the present research.

(*R*)-Oxiranecarbonitrile $\rightleftharpoons$ (*S*)-Oxiranecarbonitrile

$$\Delta_R H_0^0 = -2.4 \times 10^{-13} \text{ J mol}^{-1}$$

(*R*)-Aziridine-2-carbonitrile $\rightleftharpoons$ (*S*)-Aziridine-2-carbonitrile

$$\Delta_R H_0^0 = +8.0 \times 10^{-14} \text{ J mol}^{-1}$$

For the three aziridine-2-carbonitrile structures, $\Delta_R H_0^0$ ranges from $+8.0 \times 10^{-14}$ J mol^{-1} to $+1.1 \times 10^{-13}$ J mol^{-1}, with the *cis*-isomer yielding the smallest values and the *trans*-isomer providing the largest. Although these reaction enthalpies are smaller than those typically encountered by chemists, it can be stated with confidence that, in these precursor molecules, $\Delta_R H_0^0$ is significantly different from zero (exactly zero would be the parity-conserving result). Again, it is emphasized that these values are estimated to be correct in sign and accurate at least to within the order of magnitude. The latter estimate depends upon the behavior of the enthalpies as a function of slight changes in structure and basis set size, as well as on previous experience with the quality of the RPA compared to more rigorous approaches [23]. Clearly experimental tests would be highly desirable [3][6][73].

Obviously the reaction enthalpies for enantiomerization are exceedingly small compared to more familiar examples, such as the present prediction of the *cis*/*trans*-isomerization of aziridine-2-carbonitrile.

cis-Aziridine-2-carbonitrile $\rightleftharpoons$ *trans*-Aziridine-2-carbonitrile

$$\Delta_R H_0^0 = (3.7 \pm 2.0) \text{ kJ mol}^{-1}$$

The estimate of uncertainty is based upon experience with the performance of similar theoretical methods on other molecules. The differences between these reaction enthalpies span about 16 orders of magnitude. One may question whether the small ΔE_{pv} could have had any biochemical consequences at ordinary temperatures. The short preliminary answer to this inquiry is that, at present, one cannot exclude such a possibility, although a definitive conclusion does not seem likely in the near future. The present work is one, albeit small, contribution towards such an answer.

We acknowledge the stimulation of our interest in these biochemical precursor molecules by *Albert Eschenmoser* many years ago, to whom this paper is justly dedicated. The authors also enjoyed helpful discussions on many aspects with *T.-K. Ha* and *J. Stohner*, as well as *A. Bauder* and *F. Müller* on microwave spectra of these molecules. This work was supported financially by the *ETH*-Zürich (including C4 and CSCS), as well as by the *Swiss National Science Foundation* and by the *Deutsche Forschungsgemeinschaft* (fellowship to *R.B*).

Appendix

Table 1A. *Cartesian Coordinates* (in Å) *of the Optimized Oxiranecarbonitrile (CH_2OCHCN) Structure*

Atom	*x*	*y*	*z*
RHF/DZP			
O	– 1.203750	– 0.632316	– 0.434785
C	– 1.364351	0.688102	0.008408
C	– 0.315558	– 0.179893	0.539803
H	– 1.104309	1.450961	– 0.707240
H	– 2.238650	0.873006	0.611681
H	– 0.415898	– 0.626199	1.515181
C	1.075842	0.005532	0.118604
N	2.163165	0.159813	– 0.176975
RHF/TZP			
O	– 1.200247	– 0.637487	– 0.426601
C	– 1.361270	0.685366	0.002251
C	– 0.310547	– 0.170486	0.539652
H	– 1.108189	1.439248	– 0.721771
H	– 2.232612	0.875086	0.603960
H	– 0.411984	– 0.603758	1.518112
C	1.073694	0.008438	0.117368
N	2.153632	0.156590	– 0.178465
RHF/TZ2P			
O	– 1.199148	– 0.638801	– 0.424173
C	– 1.359988	0.685692	0.000286
C	– 0.310560	– 0.168753	0.539794
H	– 1.106534	1.434366	– 0.724126
H	– 2.228180	0.875757	0.600692
H	– 0.411342	– 0.596592	1.516864
C	1.074245	0.008823	0.116594
N	2.150333	0.155785	– 0.178521
RHF/TZ2P(*f*,*d*)			
O	– 1.197705	– 0.635481	– 0.425651
C	– 1.359712	0.683091	0.002718
C	– 0.310689	– 0.170613	0.537539
H	– 1.108473	1.437111	– 0.718808
H	– 2.229336	0.872091	0.603649
H	– 0.410662	– 0.603203	1.514265
C	1.073111	0.008542	0.116704
N	2.149706	0.156602	– 0.177483
MP2/DZP			
O	– 1.227966	– 0.670366	– 0.422251
C	– 1.369217	0.708911	– 0.023890
C	– 0.317019	– 0.149381	0.564436
H	– 1.084420	1.440418	– 0.779746
H	– 2.249828	0.933919	0.577587
H	– 0.444584	– 0.547964	1.571252
C	1.069692	0.008860	0.136628
N	2.202954	0.147188	– 0.196530

Table 1A. *(cont.)*

Atom	*x*	*y*	*z*
MP2/TZP			
O	– 1.221463	– 0.679307	– 0.408054
C	– 1.360142	0.705008	– 0.035580
C	– 0.309984	– 0.133019	0.565385
H	– 1.081984	1.416543	– 0.804936
H	– 2.237629	0.938504	0.557000
H	– 0.439505	– 0.507634	1.574617
C	1.064611	0.015877	0.136571
N	2.184656	0.139199	– 0.200439
MP2/TZ2P			
O	– 1.221001	– 0.681944	– 0.405026
C	– 1.359575	0.707400	– 0.037776
C	– 0.308519	– 0.130542	0.567025
H	– 1.079701	1.409122	– 0.807927
H	– 2.232217	0.938576	0.553195
H	– 0.438339	– 0.500178	1.572214
C	1.066008	0.014508	0.132919
N	2.180551	0.139202	– 0.199631
MP2/TZ2P(*f*,*d*)			
O	– 1.215222	– 0.670422	– 0.413135
C	– 1.355774	0.702646	– 0.029012
C	– 0.310091	– 0.140822	0.562403
H	– 1.075196	1.419298	– 0.786605
H	– 2.230721	0.927340	0.563116
H	– 0.440079	– 0.524526	1.563557
C	1.061267	0.011961	0.134430
N	2.175799	0.142938	– 0.196837

Table 2A. *Cartesian Coordinates* (in Å) *of the Optimized* cis-*Aziridine-2-carbonitrile ($CH_2NHCHCN$)*

Atom	*x*	*y*	*z*
RHF/DZP			
N	– 1.295876	0.756721	0.181984
C	– 1.353341	– 0.686706	0.205310
C	– 0.317938	0.015573	– 0.590805
H	– 0.898739	1.134549	1.020764
H	– 2.190116	– 1.125672	– 0.310811
H	– 1.030297	– 1.206325	1.092572
H	– 0.409456	0.096470	– 1.659712
C	1.064746	– 0.036761	– 0.123744
N	2.141580	– 0.070849	0.244133
RHF/TZP			
N	1.292549	– 0.758890	0.169819
C	1.352293	0.681547	0.210612
C	0.311973	– 0.005117	– 0.586093
H	0.902973	– 1.147165	1.005531
H	2.185264	1.125132	– 0.302944
H	1.039226	1.187715	1.106339
H	0.403084	– 0.071887	– 1.653758
C	– 1.063301	0.039370	– 0.119945
N	– 2.133619	0.066758	0.243572
RHF/TZ2P			
N	1.288458	– 0.760828	0.168585
C	1.351196	0.680030	0.213486
C	0.312527	– 0.001575	– 0.587514
H	0.893639	– 1.145478	0.999322
H	2.184569	1.120458	– 0.295785
H	1.037281	1.181842	1.107316
H	0.404878	– 0.065552	– 1.651791
C	– 1.063289	0.041529	– 0.121849
N	– 2.128340	0.065295	0.244910
RHF/TZ2P(*f*,*d*)			
N	1.287613	– 0.758589	0.168369
C	1.350285	0.678880	0.212593
C	0.312326	– 0.002497	– 0.586240
H	0.899027	– 1.151484	0.998702
H	2.184449	1.121334	– 0.296029
H	1.036696	1.183375	1.106453
H	0.403637	– 0.067101	– 1.652009
C	– 1.062044	0.041126	– 0.121223
N	– 2.127858	0.065544	0.244406
MP2/DZP			
N	– 1.318120	0.777957	0.181883
C	– 1.357962	– 0.698465	0.221862
C	– 0.321870	0.003040	– 0.601404
H	– 0.867202	1.126293	1.032252
H	– 2.205201	– 1.145566	– 0.292781
H	– 1.014652	– 1.211020	1.119197
H	– 0.445291	0.071492	– 1.680395
C	1.056630	– 0.042545	– 0.143489
N	2.178377	– 0.062148	0.253499

Table 2A. *(cont.)*

Atom	*x*	*y*	*z*
MP2/TZP			
N	1.309913	– 0.780628	0.163337
C	1.351973	0.689112	0.232612
C	0.314337	0.014656	– 0.597055
H	0.866180	– 1.148364	1.006524
H	2.195997	1.142572	– 0.269706
H	1.017347	1.177093	1.140133
H	0.437715	– 0.030585	– 1.671285
C	– 1.052112	0.048233	– 0.139823
N	– 2.161365	0.054096	0.253994
MP2/TZ2P			
N	1.305045	– 0.784404	0.164372
C	1.353673	0.689504	0.234010
C	0.313264	0.017361	– 0.599861
H	0.852393	– 1.138077	1.000670
H	2.196840	1.132705	– 0.268472
H	1.019460	1.174399	1.137005
H	0.439575	– 0.029957	– 1.668361
C	– 1.053167	0.049076	– 0.139953
N	– 2.155487	0.054618	0.254625
MP2/TZ2P(*f*,*d*)			
N	1.299236	– 0.779016	0.167966
C	1.347765	0.686574	0.232247
C	0.315078	0.013436	– 0.599690
H	0.846264	– 1.137294	1.003138
H	2.193777	1.130999	– 0.266722
H	1.008659	1.177844	1.131150
H	0.442439	– 0.035982	– 1.669197
C	– 1.047502	0.048015	– 0.141599
N	– 2.149791	0.056262	0.253985

Table 3A. *Cartesian Coordinates* (in Å) *of the Optimized* cis/trans-*Aziridine-2-carbonitrile ($CH_2NHCHCN$) Transition Structure*

Atom	*x*	*y*	*z*
RHF/DZP			
N	– 1.266828	– 0.663836	– 0.265705
C	– 1.378251	0.719718	– 0.136406
C	– 0.312195	– 0.101280	0.570819
H	– 1.606287	– 1.507211	– 0.655741
H	– 1.064875	1.349174	– 0.958573
H	– 2.173033	1.128142	0.474303
H	– 0.380453	– 0.241519	1.640160
C	1.081315	0.001461	0.106469
N	2.164852	0.080173	– 0.233804
RHF/TZP			
N	– 1.263053	– 0.663164	– 0.261748
C	– 1.376335	0.715968	– 0.136510
C	– 0.306784	– 0.099023	0.567123
H	– 1.600863	– 1.503967	– 0.649552
H	– 1.069672	1.343356	– 0.959702
H	– 2.167079	1.124402	0.475422
H	– 0.376317	– 0.234765	1.634707
C	1.079307	0.002933	0.104369
N	2.155749	0.079488	– 0.232758
RHF/TZ2P			
N	– 1.262091	– 0.662442	– 0.262403
C	– 1.374968	0.716674	– 0.136117
C	– 0.306448	– 0.100728	0.567388
H	– 1.599762	– 1.500046	– 0.648948
H	– 1.066523	1.342443	– 0.955378
H	– 2.161837	1.123005	0.476332
H	– 0.376342	– 0.234937	1.631581
C	1.079820	0.002453	0.103952
N	2.152204	0.079930	– 0.232501
RHF/TZ2P(*f*,*d*)			
N	– 1.261205	– 0.662719	– 0.260429
C	– 1.374381	0.714410	– 0.136934
C	– 0.306417	– 0.097739	0.565925
H	– 1.598803	– 1.502315	– 0.645215
H	– 1.069221	1.340279	– 0.959118
H	– 2.163027	1.123460	0.473751
H	– 0.375010	– 0.230783	1.631859
C	1.078780	0.003238	0.103829
N	2.151794	0.078898	– 0.232249
MP2/DZP			
N	– 1.280012	– 0.666637	– 0.278100
C	– 1.388740	0.732020	– 0.140684
C	– 0.317413	– 0.112190	0.582424
H	– 1.630960	– 1.516856	– 0.682727
H	– 1.046704	1.373066	– 0.958691
H	– 2.189135	1.146787	0.479663
H	– 0.412102	– 0.248806	1.663864
C	1.073993	– 0.000789	0.125554
N	2.201678	0.081867	– 0.244185

Table 3A. *(cont.)*

Atom	*x*	*y*	*z*
MP2/TZP			
N	– 1.271009	– 0.667589	– 0.269511
C	– 1.383267	0.724890	– 0.145339
C	– 0.310010	– 0.103960	0.578921
H	– 1.617134	– 1.517531	– 0.666959
H	– 1.048491	1.356682	– 0.966127
H	– 2.178170	1.140486	0.472030
H	– 0.407424	– 0.224996	1.656414
C	1.068922	0.003554	0.123886
N	2.183991	0.078120	– 0.243865
MP2/TZ2P			
N	– 1.272782	– 0.664295	– 0.273953
C	– 1.380602	0.730136	– 0.140687
C	– 0.308205	– 0.113038	0.579817
H	– 1.620884	– 1.506717	– 0.674254
H	– 1.038442	1.361387	– 0.951290
H	– 2.167542	1.139718	0.481062
H	– 0.406223	– 0.237843	1.651150
C	1.070022	– 0.000387	0.120396
N	2.179687	0.081351	– 0.242001
MP2/TZ2P(*f*,*d*)			
N	– 1.268838	– 0.664305	– 0.270444
C	– 1.375249	0.725441	– 0.143749
C	– 0.309501	– 0.106382	0.577856
H	– 1.616332	– 1.510465	– 0.665226
H	– 1.035650	1.354740	– 0.958639
H	– 2.164881	1.140846	0.472905
H	– 0.407055	– 0.226455	1.650914
C	1.065543	0.000875	0.121716
N	2.175447	0.078449	– 0.241855

Table 4A. *Cartesian Coordinates* (in Å) *of the Optimized* trans-*Aziridine-2-carbonitrile ($CH_2NHCHCN$) Structure.*

Atom	*x*	*y*	*z*
RHF/DZP			
N	– 1.249225	– 0.651490	– 0.435330
C	– 1.362819	0.734711	– 0.045241
C	– 0.315102	– 0.133216	0.542434
H	– 1.939968	– 1.232089	– 0.000483
H	– 1.090318	1.448713	– 0.803264
H	– 2.169523	1.032237	0.605597
H	– 0.415684	– 0.429165	1.573077
C	1.076906	– 0.016530	0.114798
N	2.168424	0.091209	– 0.188076
RHF/TZP			
N	– 1.247199	– 0.653208	– 0.430978
C	– 1.359564	0.732137	– 0.048234
C	– 0.310213	– 0.127944	0.538933
H	– 1.932366	– 1.233806	0.008751
H	– 1.094371	1.440797	– 0.810548
H	– 2.162447	1.031661	0.602375
H	– 0.413395	– 0.417508	1.568881
C	1.075284	– 0.014845	0.114012
N	2.159878	0.089066	– 0.185793
RHF/TZ2P			
N	– 1.246266	– 0.654199	– 0.429331
C	– 1.357918	0.732463	– 0.047861
C	– 0.309954	– 0.126904	0.539852
H	– 1.929400	– 1.229521	0.012525
H	– 1.092934	1.437205	– 0.809490
H	– 2.159021	1.030293	0.600186
H	– 0.412524	– 0.414624	1.566524
C	1.075913	– 0.015098	0.112826
N	2.156148	0.088942	– 0.187552
RHF/TZ2P(*f*,*d*)			
N	– 1.245484	– 0.652957	– 0.427352
C	– 1.357771	0.730733	– 0.048094
C	– 0.309691	– 0.126334	0.538306
H	– 1.928494	– 1.234804	0.007002
H	– 1.095429	1.437342	– 0.810664
H	– 2.158717	1.030708	0.601105
H	– 0.411528	– 0.412320	1.567062
C	1.075003	– 0.014891	0.112512
N	2.155815	0.088698	– 0.187359
MP2/DZP			
N	– 1.262716	– 0.670473	– 0.449117
C	– 1.367891	0.749226	– 0.055979
C	– 0.320309	– 0.124678	0.559867
H	– 1.974381	– 1.216600	0.042563
H	– 1.068455	1.452648	– 0.829324
H	– 2.185749	1.064701	0.590578
H	– 0.447336	– 0.412532	1.602805
C	1.066813	– 0.020660	0.133079
N	2.203720	0.089044	– 0.197972

Table 4A. *(cont.)*

Atom	*x*	*y*	*z*
MP2/TZP			
N	– 1.258062	– 0.671546	– 0.441672
C	– 1.358706	0.745505	– 0.059134
C	– 0.312985	– 0.117940	0.556277
H	– 1.964659	– 1.216709	0.053159
H	– 1.067382	1.439212	– 0.836490
H	– 2.170977	1.061793	0.584466
H	– 0.443255	– 0.395145	1.595738
C	1.062566	– 0.017181	0.132658
N	2.186428	0.084482	– 0.198572
MP2/TZ2P			
N	– 1.257620	– 0.673861	– 0.441582
C	– 1.358369	0.747638	– 0.059375
C	– 0.311382	– 0.117656	0.558779
H	– 1.958497	– 1.209085	0.058238
H	– 1.063547	1.433433	– 0.835518
H	– 2.168287	1.061036	0.579758
H	– 0.441495	– 0.394192	1.592675
C	1.063962	– 0.018356	0.129694
N	2.182086	0.085585	– 0.197937
MP2/TZ2P(*f*,*d*)			
N	– 1.253278	– 0.667648	– 0.442573
C	– 1.353679	0.744476	– 0.057163
C	– 0.312607	– 0.121218	0.555985
H	– 1.956792	– 1.209945	0.047444
H	– 1.058285	1.436901	– 0.828651
H	– 2.164050	1.057675	0.583133
H	– 0.443953	– 0.399241	1.590501
C	1.059579	– 0.019110	0.130648
N	2.177900	0.086198	– 0.197071

Table 5A. Ab initio *Harmonic Vibrational Spectrum of Oxiranecarbonitrile (CH_2OCHCN) Obtained at the RHF Level of Theory.* The unscaled harmonic wavenumbers (ω) are in cm^{-1}, while the corresponding double harmonic band strengths (G) are in pm^2.

Mode	DZP		TZP		TZ2P		TZ2P(*f*,*d*)	
	ω/cm^{-1}	G/pm^2	ω/cm^{-1}	G/pm^2	ω/cm^{-1}	G/pm^2	ω/cm^{-1}	G/pm^2
ν_1	3403	0.070	3367	0.055	3379	0.048	3366	0.054
ν_2	3359	0.027	3324	0.015	3338	0.015	3325	0.016
ν_3	3300	0.116	3268	0.083	3282	0.087	3269	0.089
ν_4	2600	0.058	2607	0.040	2595	0.043	2602	0.046
ν_5	1666	0.054	1659	0.038	1658	0.025	1660	0.030
ν_6	1540	0.222	1535	0.193	1530	0.192	1536	0.195
ν_7	1393	0.178	1389	0.192	1386	0.202	1393	0.202
ν_8	1297	0.032	1300	0.018	1301	0.013	1306	0.016
ν_9	1274	0.026	1277	0.032	1278	0.033	1280	0.036
ν_{10}	1205	0.114	1208	0.099	1208	0.085	1212	0.086
ν_{11}	1150	0.258	1149	0.220	1148	0.215	1150	0.220
ν_{12}	1038	1.150	1028	1.053	1017	1.034	1028	1.024
ν_{13}	1006	0.242	998	0.244	982	0.232	994	0.226
ν_{14}	850	0.411	847	0.420	843	0.416	847	0.397
ν_{15}	628	0.092	630	0.104	629	0.114	633	0.108
ν_{16}	591	0.037	598	0.037	594	0.040	597	0.040
ν_{17}	257	0.703	261	0.719	258	0.738	260	0.733
ν_{18}	243	0.427	248	0.446	245	0.489	246	0.489

Table 6A. Ab initio *Vibrational Spectrum of* cis-*Aziridine-2-carbonitrile ($CH_2NHCHCN$) Obtained at the RHF Level of Theory.* The unscaled harmonic wavenumbers (ω) are in cm^{-1}, while the corresponding double harmonic band strengths (G) are in pm^2

Mode	DZP		TZP		TZ2P		TZ2P(*f*,*d*)	
	ω/cm^{-1}	G/pm^2	ω/cm^{-1}	G/pm^2	ω/cm^{-1}	G/pm^2	ω/cm^{-1}	G/pm^2
ν_1	3807	0.069	3772	0.070	3789	0.080	3778	0.084
ν_2	3401	0.060	3365	0.051	3378	0.045	3365	0.050
ν_3	3366	0.015	3333	0.008	3346	0.010	3333	0.011
ν_4	3302	0.098	3272	0.074	3288	0.079	3274	0.079
ν_5	2586	0.181	2593	0.151	2582	0.154	2588	0.160
ν_6	1647	0.014	1643	0.013	1645	0.012	1643	0.013
ν_7	1519	0.118	1515	0.101	1514	0.107	1516	0.101
ν_8	1391	0.121	1384	0.114	1388	0.122	1385	0.107
ν_9	1370	0.174	1370	0.173	1374	0.190	1369	0.170
ν_{10}	1291	0.299	1290	0.283	1297	0.316	1293	0.285
ν_{11}	1246	0.087	1251	0.086	1254	0.080	1254	0.096
ν_{12}	1234	0.034	1236	0.034	1238	0.023	1237	0.033
ν_{13}	1121	0.042	1118	0.055	1120	0.065	1120	0.049
ν_{14}	1037	0.330	1037	0.254	1041	0.279	1037	0.245
ν_{15}	1021	0.444	1008	0.434	998	0.421	1006	0.414
ν_{16}	955	1.199	940	1.128	939	0.970	942	1.068
ν_{17}	841	0.496	835	0.528	833	0.476	836	0.496
ν_{18}	623	0.030	626	0.021	626	0.010	629	0.012
ν_{19}	592	0.035	599	0.028	597	0.018	599	0.016
ν_{20}	249	0.948	251	0.988	250	0.971	251	0.976
ν_{21}	241	0.871	245	0.906	242	0.969	243	0.962

Table 7A. Ab initio *Harmonic Vibrational Spectrum of* cis/trans-*Aziridine-2-carbonitrile ($CH_2NHCHCN$) Transition Structure Obtained at the RHF Level of Theory.* The unscaled harmonic wavenumbers (ω) are in cm^{-1}, while the corresponding double harmonic band strengths (G) are in pm^2.

Mode	DZP		TZP		TZ2P		TZ2P(*f*,*d*)	
	ω/cm^{-1}	G/pm^2	ω/cm^{-1}	G/pm^2	ω/cm^{-1}	G/pm^2	ω/cm^{-1}	G/pm^2
ν_1	3994	0.710	3979	0.652	3989	0.627	3978	0.625
ν_2	3337	0.190	3299	0.170	3314	0.162	3298	0.170
ν_3	3307	0.083	3272	0.070	3288	0.070	3273	0.071
ν_4	3248	0.268	3216	0.245	3233	0.250	3217	0.254
ν_5	2584	0.111	2591	0.088	2580	0.094	2586	0.097
ν_6	1667	0.143	1663	0.116	1667	0.098	1664	0.109
ν_7	1535	0.437	1530	0.394	1528	0.389	1531	0.395
ν_8	1405	0.269	1403	0.326	1399	0.361	1404	0.342
ν_9	1272	0.010	1277	0.004	1281	0.007	1283	0.007
ν_{10}	1252	0.004	1255	0.007	1258	0.009	1258	0.008
ν_{11}	1231	0.222	1225	0.222	1231	0.197	1229	0.196
ν_{12}	1187	0.038	1189	0.038	1190	0.032	1192	0.032
ν_{13}	1138	0.082	1138	0.069	1137	0.073	1137	0.069
ν_{14}	1054	0.106	1059	0.110	1049	0.077	1057	0.091
ν_{15}	998	0.471	987	0.442	979	0.390	988	0.386
ν_{16}	845	0.479	842	0.477	839	0.459	842	0.437
ν_{17}	638	0.018	644	0.025	642	0.040	645	0.039
ν_{18}	589	0.047	595	0.048	592	0.046	595	0.045
ν_{19}	254	0.305	258	0.324	256	0.352	257	0.356
ν_{20}	238	0.307	242	0.323	240	0.366	241	0.367
ν_{21}	963*i*	–	949*i*	–	972*i*	–	957*i*	–

Table 8A. Ab initio *Harmonic Vibrational Spectrum of* trans-*Aziridine-2-carbonitrile ($CH_2NHCHCN$) Obtained at the RHF Level of Theory.* The unscaled harmonic wavenumbers (ω) are in cm^{-1}, while the corresponding double harmonic band strengths (G) are in pm^2.

Mode	DZP		TZP		TZ2P		TZ2P(*f*,*d*)	
	ω/cm^{-1}	G/pm^2	ω/cm^{-1}	G/pm^2	ω/cm^{-1}	G/pm^2	ω/cm^{-1}	G/pm^2
ν_1	3809	0.058	3775	0.058	3793	0.069	3782	0.073
ν_2	3400	0.051	3365	0.042	3378	0.037	3364	0.042
ν_3	3352	0.027	3317	0.017	3335	0.016	3321	0.017
ν_4	3299	0.113	3269	0.088	3286	0.090	3272	0.091
ν_5	2594	0.144	2602	0.113	2590	0.116	2596	0.119
ν_6	1651	0.020	1645	0.011	1647	0.009	1645	0.011
ν_7	1546	0.106	1544	0.097	1543	0.110	1545	0.110
ν_8	1386	0.057	1385	0.079	1391	0.119	1385	0.075
ν_9	1355	0.420	1344	0.366	1349	0.421	1346	0.387
ν_{10}	1305	0.157	1308	0.151	1312	0.098	1309	0.137
ν_{11}	1250	0.005	1256	0.006	1258	0.007	1260	0.006
ν_{12}	1221	0.031	1224	0.025	1226	0.021	1225	0.027
ν_{13}	1065	0.098	1063	0.117	1063	0.126	1063	0.106
ν_{14}	1047	0.107	1037	0.067	1031	0.057	1036	0.067
ν_{15}	1007	1.071	999	0.784	1002	0.844	998	0.718
ν_{16}	977	0.656	965	0.831	962	0.611	967	0.801
ν_{17}	843	0.460	839	0.484	835	0.468	838	0.462
ν_{18}	624	0.229	628	0.256	626	0.273	629	0.272
ν_{19}	583	0.073	590	0.075	587	0.072	589	0.079
ν_{20}	255	0.210	259	0.223	257	0.230	258	0.226
ν_{21}	237	0.078	242	0.089	239	0.125	240	0.125

REFERENCES

[1] M. Bolli, R. Micura, A. Eschenmoser, *Chem. Biol.* **1997**, *4*, 309.
[2] S. F. Mason, *Nature* **1984**, *311*, 19.
[3] M. Quack, *Angew. Chem., Int. Ed.* **1989**, *28*, 571.
[4] S. F. Mason, 'Chemical Evolution: Origins of the Elements, Molecules, and Living Systems', Clarendon Press, Oxford, 1991.
[5] J. S. Siegel, *Chirality* **1998**, *10*, 24.
[6] M. Quack, *Nova Acta Leopoldina NF* **1999**, *81*, 137.
[7] W. Bonner, *Chirality* **2000**, *12*, 114; see also the more general discussion and different points of view in R. N. Zare, W. A. Bonner, P. Frank, in 'Chemistry for the 21st Century', Eds. E. Keinan and I. Schechter, to be published, 2000.
[8] E. Fischer, *Chem. Ber.* **1894**, *27*, 2985.
[9] E. Fischer, *Chem. Ber.* **1894**, *27*, 3189.
[10] Y. Yamagata, *J. Theoret. Biol.* **1966**, *11*, 495.
[11] D. W. Rein, *J. Mol. Evol.* **1974**, *4*, 15.
[12] V. S. Letokhov, *Phys. Lett.* **1975**, *53A*, 275.
[13] R. A. Hegstrom, D. W. Rein, P. G. H. Sandars, *J. Chem. Phys.* **1980**, *73*, 2329.
[14] S. F. Mason, G. Tranter, *Mol. Phys.* **1984**, *53*, 1091.
[15] A. J. MacDermott, *Croat. Chim. Acta* **1989**, *62*, 165.
[16] A. Bakasov, T.-K. Ha, M. Quack, in 'Proc. of the 4th Trieste Conference on Chemical Evolution: Physics of the Origin and Evolution of Life', J. Chela-Flores and F. Raulin, Kluwer Academic, Dordrecht, 1996, pp. 287–296.
[17] A. Bakasov, T.-K. Ha, M. Quack, *J. Chem. Phys.* **1998**, *109*, 7263.
[18] A. Bakasov, M. Quack, *Chem. Phys. Lett.* **1999**, *303*, 547.
[19] J. K. Laerdahl, P. Schwerdtfeger, *Phys. Rev. A* **1999**, *60*, 4439.
[20] H. Kiyonaga, T. Yagi, K. Morihashi, O. Kikuchi, *JCPE* **1999**, *11*, 165.
[21] O. Kikuchi, M. Wang, *Bull. Chem. Soc. Jpn.* **1990**, *63*, 2751.
[22] H. Kiyonaga, K. Morihashi, O. Kikuchi, *J. Chem. Phys.* **1998**, *108*, 2041.
[23] R. Berger, M. Quack, *J. Chem. Phys.* **2000**, *112*, 3148.
[24] A. Bakasov, T.-K. Ha, M. Quack, *J. Chem. Phys.* **1999**, *110*, 6081.
[25] R. Berger, M. Quack, *Angew. Chem.*, *ChemPhysChem* **2000**, in press.
[26] P. Lazzeretti, R. Zanasi, *Chem. Phys. Lett.* **1997**, *279*, 349.
[27] P. Lazzeretti, R. Zanasi, *Chem. Phys. Lett.* **1998**, *286*, 240.
[28] R. Zanasi, P. Lazzeretti, A. Ligabue, A. Soncini, in 'Advances in BioChirality', Eds. G. Pályi and C. Zucchi, Elsevier, Amsterdam, 1999, pp. 377–385.
[29] M.-A. Bouchiat, C. Bouchiat, *Rep. Prog. Phys.* **1997**, *60*, 1351.
[30] D. K. Kondepudi, G. W. Nelson, *Nature* **1985**, *314*, 438.
[31] A. Salam, *J. Mol. Evol.* **1991**, *33*, 105.
[32] A. Salam, *Phys. Lett.* **1992**, *288B*, 153.
[33] J. E. Dickens, W. M. Irvine, M. Ohishi, G. Arrhenius, S. Pitch, A. Bauder, F. Müller, A. Eschenmoser, *Origins Life Evol. Biosphere* **1996**, *26*, 97.
[34] A. Eschenmoser, E. Loewenthal, *Chem. Soc. Rev.* **1992**, *21*, 1.
[35] D. Müller, S. Pitsch, A. Kittaka, E. Wagner, C. E. Wintner, A. Eschenmoser, *Helv. Chim. Acta* **1990**, *73*, 1410.
[36] S. Pitch, A. Eschenmoser, B. Gedulin, S. Hui, G. Arrhenius, *Origins Life Evol. Biosphere* **1995**, *25*, 297.
[37] G. Ksander, G. Bold, R. Lattmann, C. Lehmann, T. Früh, Y.-B. Xiang, K. Inomata, H.-P. Bruser, J. Schreiber, E. Zass, A. Eschenmoser, *Helv. Chim. Acta* **1987**, *70*, 1115.
[38] S. Drenkard, J. Ferris, A. Eschenmoser, *Helv. Chim. Acta* **1990**, *75*, 1373.
[39] E. Wagner, Y.-B. Xiang, K. Baumann, J. Guck, A. Eschenmoser, *Helv. Chim. Acta* **1990**, *73*, 1391.
[40] S. Pitsch, E. Pombovillar, A. Eschenmoser, *Helv. Chim. Acta* **1994**, *77*, 2251.
[41] F. Müller, A. Bauder, *J. Mol. Spec.* **1996**, *179*, 61.
[42] A. Eschenmoser, *Origins Life Evol. Biosphere* **1997**, *27*, 535.
[43] R. Krishnamurthy, S. Pitch, G. Arrhenius, *Origins Life Evol. Biosphere* **1999**, *29*, 139.
[44] R. Krishnamurthy, G. Arrhenius, A. Eschenmoser, *Origins Life Evol. Biosphere* **1999**, *29*, 333.
[45] M. Diefenbach, M. Brönstrup, M. Aschi, D. Schröder, H. Schwarz, *J. Am. Chem. Soc.* **1999**, *121*, 10614.

[46] M. J. Frisch, G. W. Trucks, H. B. Schlegel, P. M. W. Gill, B. G. Johnson, M. A. Robb, J. R. Cheeseman, T. Keith, G. A. Petersson, J. A. Montgomery, K. Raghavachari, M. A. Al-Laham, V. G. Zakrzewski, J. V. Ortiz, J. B. Foresman, J. Cioslowski, B. B. Stefanov, A. Nanayakkara, M. Challacombe, C. Y. Peng, P. Y. Ayala, W. Chen, M. W. Wong, J. L. Andres, E. S. Replogle, R. Gomperts, R. L. Martin, D. J. Fox, J. S. Binkley, D. J. Defrees, J. Baker, J. P. Stewart, M. Head-Gordon, C. Gonzalez, J. A. Pople, GAUSSIAN 94, Revision C.3, Gaussian, Inc., Pittsburgh, PA 15106, U.S.A., 1995.
[47] S. Huzinaga, *J. Chem. Phys.* **1965**, *42*, 1293.
[48] T. H. Dunning, *J. Chem. Phys.* **1970**, *53*, 2823.
[49] T. H. Dunning, *J. Chem. Phys.* **1971**, *55*, 716.
[50] S. Huzinaga, *J. Chem. Phys.* **1965**, *42*, 1293.
[51] T. Helgaker, H. J. Aa. Jensen, P. Jørgensen, J. Olsen, K. Ruud, H. Ågren, T. Andersen, K. L. Bak, V. Bakken, O. Christiansen, P. Dahle, E. K. Dalskov, T. Enevoldsen, B. Fernandez, H. Heiberg, H. Hettema, D. Jonsson, S. Kirpekar, R. Kobayashi, H. Koch, K. V. Mikkelsen, P. Norman, M. J. Packer, T. Saue, P. R. Taylor, O. Vahtras, Dalton: An electronic structure program, Release 1.0, 1997.
[52] C. L. Janssen, E. T. Seidl, G. E. Scuseria, T. P. Hamilton, Y. Yamaguchi, R. B. Remington, Y. Xie, G. Vacek, C. D. Sherrill, T. D. Crawford, J. T. Fermann, W. D. Allen, B. R. Brooks, G. B. Fitzgerald, D. J. Fox, J. F. Gaw, N. C. Handy, W. D. Laidig, T. J. Lee, R. M. Pitzer, J. E. Rice, P. Saxe, A. C. Scheiner, H. F. Schaefer, PSI 2.0.8, PSITECH, Inc., Watkinsville, GA30677, U.S.A., 1995; this program is generally available for a handling fee of $100.
[53] K. V. Mikkelsen, E. Dalgaard, P. Swanstrøm, *J. Phys. Chem*. **1987**, *91*, 3081.
[54] R. S. Cahn, C. Ingold, V. Prelog, *Angew. Chem., Int. Ed*. **1966**, *5*, 385.
[55] R. D. Brown, P. D. Godfrey, A. L. Ottrey, *J. Mol. Spec*. **1980**, *82*, 73.
[56] I. Mills, T. Cvitaš, K. Homann, N. Kallay, K. Kuchitsu, 'Quantities, Units and Symbols in Physical Chemistry', 2nd edn., Blackwell Scientific Publications, Oxford, Oxford, 1993, 3rd edn. in preparation
[57] M. Quack, *J. Mol. Struct*. **1995**, *347*, 245.
[58] M. Quack, *Ann. Rev. Phys. Chem*. **1990**, *41*, 839.
[59] R. E. Carter, T. Drakenberg, N.-Å. Bergman, *J. Am. Chem. Soc*. **1975**, *97*, 6990.
[60] A. L. L. East, W. D. Allen, *J. Chem. Phys.* **1993**, *99*, 4638.
[61] W. D. Allen, A. L. L. East, A. G. Császár, in 'Structures and Conformations of Non-Rigid Molecules', Eds. J. Laane, M. Dakkouri, B. van der Veken, and H. Oberhammer, Kluwer, Dordrecht, 1993.
[62] A. G. Császár, W. D. Allen, H. F. Schaefer, *J. Chem. Phys.* **1998**, *108*, 9751.
[63] G. Tarczay, A. G. Császár, W. Klopper, V. Szalay, W. D. Allen, H. F. Schaefer, *J. Chem. Phys.* **1999**, *110*, 11971.
[64] I. M. B. Nielsen, *J. Phys. Chem. A* **1998**, *102*, 3193.
[65] P. George, C. W. Bock, J. P. Glusker, *J. Phys. Chem*. **1992**, *96*, 3702.
[66] R. S. Mulliken, *J. Chem. Phys.* **1955**, *23*, 1833.
[67] R. S. Mulliken, *J. Chem. Phys.* **1955**, *23*, 1841.
[68] R. S. Mulliken, *J. Chem. Phys.* **1955**, *23*, 2338.
[69] R. Ellerbrock, P. Rademacher, *J. Mol. Struct*. **1992**, *265*, 93.
[70] D. Felix, A. Eschenmoser, *Angew. Chem*. **1968**, *80*, 197.
[71] M. Quack, J. Stohner, *Phys. Rev. Lett*. **2000**, *84*, 3807.
[72] M. Quack, J. Stohner, *Zeitschr. Phys. Chem*. **2000**, *214*, 675.
[73] M. Quack, *Chem. Phys. Lett*. **1986**, *132*, 147.
[74] H. Hollenstein, D. Luckhaus, J. Pochert, M. Quack, G. Seyfang, *Angew. Chem., Int. Ed.* **1997**, *36*, 140.
[75] R. Berger, M. Quack, J. Stohner, in preparation.

Received May 2, 2000